JOURNAL OF PETROLOGY | VOLUME 40 | NUMBER 5 | PAGES 807–830 | 1999

400 my of Basic Magmatism in a Single Lithospheric Block during Cratonization: Ion Microprobe Study of Plagioclase Megacrysts in Mafic Rocks from Transbaikalia, Russia

ILYA N. BINDEMAN[1]*, ANDREW M. DAVIS[1,2] AND STEPHEN M. WICKHAM[3]

[1]DEPARTMENT OF THE GEOPHYSICAL SCIENCES, UNIVERSITY OF CHICAGO, 5734 SOUTH ELLIS AVENUE, CHICAGO, IL 60637, USA

[2]ENRICO FERMI INSTITUTE, UNIVERSITY OF CHICAGO, 5640 SOUTH ELLIS AVENUE, CHICAGO, IL 60637, USA

[3]GALSON SCIENCES LIMITED CO. 5, GROSVENOR HOUSE, MELTON ROAD, OAKHAM LE15 6AX, UK

RECEIVED MAY 1, 1998; REVISED TYPESCRIPT ACCEPTED NOVEMBER 17, 1998

Following accretion of southern Siberian microcontinents to the Siberian craton in the Early Paleozoic, five cycles of K-rich silicic magmatism, progressively decaying in volume, occurred on batholithic scales throughout the Paleozoic and Early Mesozoic, followed by rift-related alkali volcanism of Jurassic to Recent age. Most of the post-Ordovician magmatism occurred within the Ordovician accreted terrane of Transbaikalia, during its 400 my of cratonization. Basic magmas may be critical in the generation of K-rich silicic magma, yet only subordinate volumes of coeval mafic rocks in the silicic plutons and synchronous volcanics are present. Most of the mafic rocks contain plagioclase megacrysts (1–5 mm), and these were used to reconstruct the primary basic magma chemistry and its evolution with time. Optical and scanning electron microscopy studies, and electron microprobe profiling through plagioclase megacrysts of different ages revealed unzoned, Ca-rich cores in a number of crystals in each sample. Several crystals within each rock in a number of rocks within each age group were studied. Several ion microprobe analyses inside each of these cores were made for concentrations of Li, Be, B, F, Mg, P, Cl, K, Ti, Fe, Co, Rb, Sr, Y, Zr, Nb, Cs, Ba, La, Ce, Pr, Nd, Sm, Eu, and Pb. In addition, partition coefficients for the same trace elements and the relevant compositional range of plagioclase were used to convert trace element concentrations in Transbaikalian plagioclase to parental magmatic values. Whole-rock and whole-plagioclase analyses for oxygen isotopes and trace elements were also made to constrain the amount of contamination of basic magma and study its temporal trends. Plagioclase core compositions reveal up to one order of magnitude variation of some trace elements and ratios between suites, and show a progressive change in trace element concentration with decreasing age. Plagioclase megacrysts and the reconstructed basic magmas exhibit depletion in large ion lithophile elements, volatile elements, light rare earth elements and $\delta^{18}O$, and simultaneous increase in high field strength elements and K. We speculate on tectonic implications of the established chemical trends as reflecting progressive incompatible element depletion and devolatilization of a mantle source and increasing prevalence of alkali basalt from the sublithospheric mantle in the course of cratonization.

KEY WORDS: *anorogenic; cratonization; ion microprobe; stable isotopes; trace elements*

INTRODUCTION

Secondary ion mass spectrometry studies of liquidus phases

Ion microprobe analysis provides a local, sensitive and minimally destructive method to study the composition

*Corresponding author. Present address: Department of Geology and Geophysics, The University of Wisconsin–Madison, 1215 West Dayton Street, Madison, WI 53706, USA. Telephone: 608-263-5659. Fax: 608-262-0693. e-mail: inbindem@geology.wisc.edu

and micron-scale zoning of trace elemental composition of minerals at ppm levels of concentration (Shimizu & Hart, 1982; Zinner & Crozaz, 1986). Knowledge of appropriate partition coefficients leads to characterization of the primary composition of the parental melt from which these minerals had crystallized. The use of the 'recorded' trace element concentrations in phenocrysts can be used to infer the trace elemental evolution of magmas, and then infer magma chamber processes such as fractionation and magma mixing (Blundy & Shimizu, 1991; Singer *et al.*, 1995; Bindeman, 1998). In complement to trace elements, isotope profiling of phenocrysts provides further insight into changes of magma sources during phenocryst growth history (Davidson & Tepley, 1998).

The reconstruction of the parental melt composition based on unzoned surviving relict phenocryst cores is particularly important for old, variously differentiated, altered and tectonized rocks, in which study of melt inclusions is problematic. This approach may be the only way for plutonic rocks which may represent cumulates, residual melts or hybrid rocks for which bulk-rock studies are of limited compositional significance. Unzoned cores of relict phenocrysts allow us to see back through the effects of fractional crystallization, magma mixing and subsolidus alteration of the rock. This approach has more promise for mafic rocks, in which accessory minerals (which may have high trace element concentrations) are not normally present or appear only during later stages of crystallization after phenocrysts.

Plagioclase megacrysts approach

The use of plagioclase as a recorder of the liquidus chemistry of magma has the following advantages: (1) It is common in most igneous rocks. (2) It appears as a liquidus phase in most basaltic magmas. (3) Minerals that sometimes crystallize before plagioclase (e.g. olivine, pyroxenes) do not normally fractionate trace elements significantly and, therefore, plagioclase adequately reflects the initial trace element signature of their parental magma. (4) Plagioclase contains measurable quantities of trace elements of different geochemical groups [e.g. large ion lithophile elements (LILE), rare earth elements (REE), high field strength elements (HFSE)]. (5) It has very low diffusivities of major and trace cations of all of these groups (diffusion coefficient values at 1000°C are typically 10^{-15}–10^{-19} m^2/s) (Cherniak & Watson, 1992; Giletti, 1994; Brady, 1995; Giletti & Shanahan, 1997) and high closure temperatures (>800–1000°C for 1 mm size crystal at 1000°C per 1 my cooling) (Cherniak & Watson, 1992; Cherniak, 1995) in comparison with Fe–Mg igneous minerals. Diffusion in anorthite is 3–4 orders of magnitude slower than in albite (Giletti, 1994). Therefore, plagioclase, especially calcic plagioclase, preserves its initial composition in most cases.

The central assumption in using plagioclase to retrieve the composition of parental melt is that the large (>1 mm) and unzoned Ca-rich cores of plagioclase preserve the original concentration of trace elements, inherited from the parental high-temperature basaltic magma from which they crystallized. Rims over the existing core are often the result of overgrowth, which is often perceived to be the outcome of volcanic eruption or plutonic intrusion into the cold country rocks or into a colder magma ('plutonic quenching'). As a result, crystallization of new layers on plagioclase cores proceeds and newly grown rims encapsulate the pre-existing core, and isolate it from further interaction with the melt.

One can argue that if a plateau is found on the concentration–distance plot, the concentrations of trace elements in crystals are magmatic and were not modified irregularly as expected for subsolidus alterations. The presence of low-amplitude oscillatory zoning even in the Archean plagioclase cores demonstrates that the original magmatic, micron-scale liquidus features were not obliterated later (e.g. Morse, 1984). Large size and uniformity of the cores suggest formation in large, slowly cooling, and high-temperature reservoirs of basic magma. In contrast to extremely sluggish cation diffusion in feldspars, they have shown a greater susceptibility to oxygen isotope exchange (e.g. Criss & Taylor, 1986). Below we use an additional test for the preservation of magmatic values of feldspars and retention of their high-temperature isotopic fractionation with other minerals.

In addition, surviving plagioclase cores serve as a good container of near-liquidus trace elements even if their host basic magma suffered subsequent fractionation and/or assimilation of crustal rocks. The use of near-liquidus phenocrysts, hence, aims to minimize the possible effects of assimilation and fractionation. This is the best one can do for basic rocks in an attempt to take one step back toward the 'primary', mantle-equilibrated composition.

An application to long-term magmatic evolution during cratonization

The transformation of orogenic belts into cratonic regions occurs by means of a series of interrelated magma–tectonic processes: erosion and uplift, decrease of volumes of magmatism with time, and change of the character of magmatism toward more alkalic, and especially K-rich compositions (e.g. Windley, 1984, 1993; Pollack, 1986; Bonin, 1987). Studies of areas characterized by Proterozoic cratonization—the Arabian–Nubian Shield (Abdel-Rahman, 1995), NE Brazil (Dal'Agnol *et al.*, 1987), Fennoscandia (Ramo, 1991) and the USA (Windley, 1984; Anderson & Morrison, 1992)—show that rocks

formed in these areas are characterized by specific trace elemental concentrations and ratios. Phanerozoic magmatism in Transbaikalia since 400 Ma is probably the youngest and best-exposed example of modern cratonization reflecting a transition from orogenic to anorogenic magmatism.

Current petrogenetic models call for basaltic magma to provide both heat and matter for anorogenic granitoids (e.g. Barker *et al.*, 1975; Wickham *et al.*, 1995, 1996). Melting of thickened lithospheric mantle is considered to supply the basaltic magma into the lower crust, which causes underplating, melting, hybridization and production of granitic, syenitic and monzonitic magmas with clear anorogenic trace element affinities (Pollack, 1986; Bonin, 1987; Wickham *et al.*, 1996). The heat and chemical composition of basic magmas are therefore critical, yet only subordinate volumes of mafic rocks are present in silicic plutons. Silicic rocks are well exposed on the surface and can be easily studied by whole-rock methods, but this is not the case with their mafic counterparts. The silicic plutons serve as traps and density filters, rarely allowing the dense basic magma to reach the surface (e.g. Bonin, 1987). In addition, the mafic rocks are often highly altered, fractionated and hybridized, which complicates the interpretation of whole-rock analyses.

Here we use plagioclase megacryst cores in the mafic rocks to unravel the chemical compositions of their parental melts. In combination, oxygen isotope study of whole rocks and minerals, and whole-rock chemical compositions allow assessment of the effects of fractionation, assimilation and secondary alteration. Thus, on the basis of ion microprobe-measured trace element concentrations in cores of plagioclase it is possible to document the evolution of primary basic magma chemistry during the process of cratonization in a single lithospheric block. Unzoned cores of phenocrysts allow us to see back through the effects of fractional crystallization, magma mixing and subsolidus alteration of the rock, and retain compositional information on the parental melt composition. We describe the technique for selecting suitable crystals for analysis. Given the narrow compositional range of Transbaikalian plagioclase of different ages (see below), this procedure leads to direct characterization of the relative trace element enrichment or depletion history, by comparing the composition of selected plagioclases. This, in combination with oxygen isotope studies, provides insight into the mantle source regions and their evolution.

REGIONAL BACKGROUND

Geology

Province

The granitoid province of Transbaikalia is a vast area of Phanerozoic granitic magmatism in Siberia (Fig. 1), east and south of the Siberian craton and Lake Baikal. The concentration of igneous rocks in this territory is enormous, as can be seen from regional and local maps (see Fig. 1a and b). The geology of the area was recently reviewed in the English geological literature by Wickham *et al.* (1995, 1996). The province consists of several magmatic belts (see Fig. 1): (1) Ordovician–Silurian Angaro-Vitim batholith; (2) Devonian–Carboniferous plutonic belt; and (3) Early Permian, (4) Late Permian, and (5) Permo–Triassic plutonic belts with contemporaneous volcanics. Igneous activity continued through the Mesozoic and Tertiary to the present day and comprises five additional volcanic–plutonic suites, considered here: (6) Middle to Late Jurassic; (7) Early Cretaceous; (8) Late Cretaceous; (9) Tertiary; (10) Early Quaternary. The last two suites are entirely volcanic and directly related to the opening of the Baikal Rift (Rasskazov, 1994).

The areas of plutonic rocks of different ages decrease with decreasing age, total outcrop areas for plutonic suites (1)–(5) of Transbaikalia and the adjacent areas of northern Mongolia being: (1) 150 000 km^2; (2) 39 000 km^2; (3) 25 000 km^2; (4) 7800 km^2; (5) 5600 km^2 (Litvinovsky & Zanvilevich, 1998). Exposed volcanic areas also decrease with time, but it is difficult to make quantitative estimates. Overall decrease of the exposed surface areas of magmatic rocks of each age group is likely to reflect the decrease of magma volumes during the last 400 my.

Transbaikalian magmatism bears many features collectively attributed to orogenic to postorogenic and then to anorogenic magmatic transitions (Leontiev *et al.*, 1981; Zanvilevich *et al.*, 1985). For example, postorogenic and anorogenic magmatism is predominantly silicic with only subordinate volumes of mafic rocks. In contrast, extensive mafic–silicic hybridization textures in outcrops (e.g. Litvinovsky *et al.*, 1994; Bindeman, 1998) and isotopic and trace elemental studies (Wickham *et al.*, 1995, 1996) show conspicuous involvement of basic magma in the petrogenesis.

Tectonic and magmatic evolution

Tectonic histories of the region of southern Siberia and Mongolia were recently reviewed by Zonenshain *et al.* (1990) and Sengor & Natal'in (1996). Following the accretion of several microcontinents to the southern margin of the Siberian platform in the Lower Paleozoic, Transbaikalia and Northern Mongolia developed as an intracratonic region. The Ordovician–Silurian magmatism was characterized by emplacement of the exceptionally large Angaro–Vitim batholith, a slab-shaped body 10–15 km thick and originally covering an area of >200 000 km^2 (Litvinovsky *et al.*, 1994). At the present-day erosional level, the lower parts of this pluton are partly exposed. Younger magmatic suites (2)–(10), considered here, reside inside this batholith (see Fig. 1).

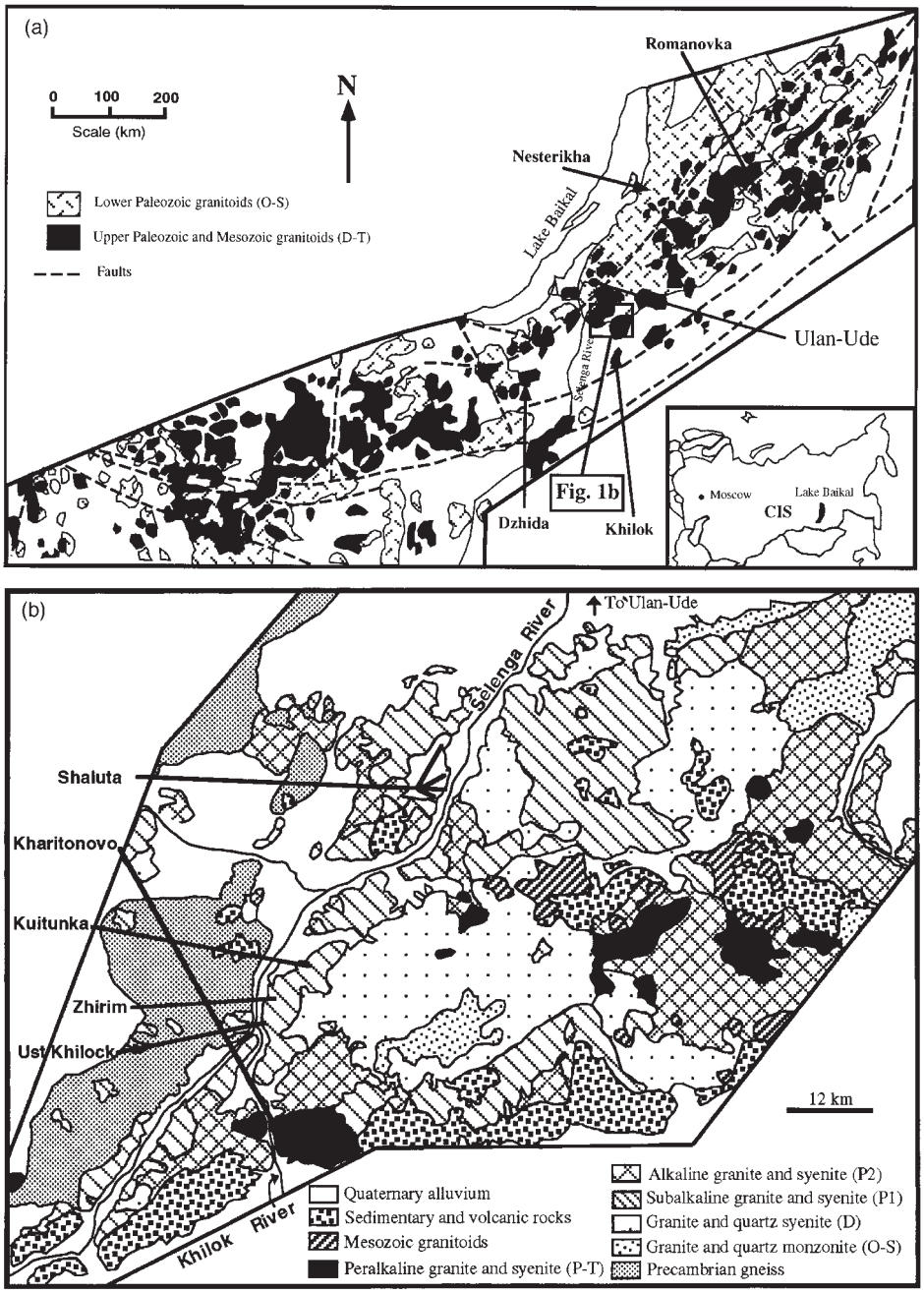

Fig. 1. (a) Map of Transbaikalia with the position of Lower Selenga Plutonic Complex (LSPC) and other sample localities. (b) Lower Selenga Plutonic Complex and localities with mafic rock occurrences. It should be noted that igneous rocks constitute ~90% of the territory.

Most of the Paleozoic post-collisional geological history can be interpreted as successive accretions of microcontinents or island arcs and geometrical expansion of the southern margin of the craton to the south-east while Transbaikalia and Northern Mongolia became increasingly remote from plate boundaries (Gordienko, 1987). Several recent tectonic models propose closure of the Mongol–Okhotsk ocean to the south by anticlockwise rotation of the Chinese blocks as a result of strike-slip faulting and shortening (Sengor & Natal'in, 1996; Nie *et al.*, 1990).

The Mesozoic and Cenozoic geological history started with the closure of the Mongol–Okhotsk ocean in Late Jurassic time. Since then, magmatism has traced

Table 1: Age of magmatic suites of Transbaikalia

Geological age	Absolute age (Ma)	Method	Reference
(1) Ordovician–Silurian	506–426	U–Pb	Neymark *et al.*, 1993
(2) Devonian–Carboniferous		U–Pb	Bowring *et al.*, in preparation
(3) Early Permian	290–240	Rb–Sr, K–Ar	Zanvilevich & Litvinovsky, 1991
(4) Late Permian	276–228	U–Pb	Wickham *et al.*, 1995
(5) Permo-Triassic	220	Rb–Sr	Zanvilevich & Litvinovsky, 1991
	192	U–Pb	Bowring *et al.*, in preparation
(6) Middle to Late Jurassic	162–133	K–Ar	Rasskazov, 1994
	159	K–Ar	Rasskazov, 1994
(7) Early Cretaceous	120–113	K–Ar	Kononova *et al.*, 1993
	120–100	K–Ar	Rasskazov, 1994
(8) Late Cretaceous–Paleogene	61–29	K–Ar	Rasskazov, 1994
(9) Tertiary	23–10	K–Ar	Rasskazov, 1994
(10) Recent	7–0	K–Ar	Rasskazov, 1994

intracontinental rift tectonics, which culminated in the opening of the Baikal rift during the Tertiary (Rasskazov, 1993, 1994).

The main conclusion regarding the tectonic evolution of Transbaikalia is that magmatism occurred in the same lithospheric block as occupied by the Angaro–Vitim batholith of Ordovician–Silurian age (see Fig. 1). No major deformation or regional metamorphism is known since the last collisional event in Ordovician–Silurian.

Age of magmatism

The existing ages result from radiometric dating, paleontological information, and structural–intraplutonic relations (Table 1). They are based on extensive large-scale and small-scale mapping by various groups of Soviet/Russian geologists during the 1960s to 1990s. Sm–Nd, U–Pb, and Rb–Sr radiometric dating of different plutonic belts is currently under way in several laboratories.

The relative ages of Paleozoic and Mesozoic plutonic complexes are constrained by geological cross-cutting relations (Leontiev *et al.*, 1981; Zanvilevich *et al.*, 1985; Gordienko, 1987). Mesozoic volcanic suites are dated using both paleontological and structural information (Rasskazov, 1993). Existing radiometric age determinations are consistent with the relative age sequence (Table 1). Many Mesozoic and Cenozoic volcanic rocks have been dated by the K–Ar method [see Table 1 and Kononova *et al.* (1993) and Rasskazov (1993, 1994), and references therein].

Coeval silicic and basic magmatism

The age of mafic rocks associated with granitic plutons is constrained mainly by their structural relations with silicic rocks. For example, liquid–liquid, crenulated contact zones occur between many mafic and silicic rocks (Litvinovsky *et al.*, 1994; Bindeman, 1998). Mafic rocks have finely crystalline ('chilled') margins against the silicic host, and are also intruded by the silicic host residual melt. Such field relationships have long been interpreted as reflecting a close time and space association of two magmas (e.g. Furman & Spera, 1985; Frost & Mahood, 1987).

Two main types of coeval plutonic relations are present in Transbaikalia and elsewhere in the world: (1) thin (up to several meters thick) synplutonic dikes; (2) composite dikes formed by coeval intrusion of silicic and basic magma through the same fracture (e.g. Frost & Mahood, 1987). Mafic rocks in composite dikes in Transbaikalia occur as large enclaves with chilled margins, often oriented parallel to the walls of the fracture. Some synplutonic dikes change into composite dikes along their strike.

Both synplutonic and composite dikes reflect late-plutonic rapid intrusion and chilling of basic and/or basic + silicic magmas. Textures are consistent with the basic magma becoming >50% crystalline during initial rapid cooling and encapsulation of phenocrysts by the groundmass crystals. This, combined with the small volume of basic magma, leads to quenching of the plagioclase megacrysts in them to near the closure temperature. Therefore, plutonic quenching of plagioclase megacrysts proceeds similarly to volcanic quenching, and homogeneous near-liquidus cores are preserved in both cases.

Sampling strategy

Samples considered in this study were collected within a terrane that has remained as a single lithospheric block

for the last 400 my (see Fig. 1a). Our collection of mafic rocks is as extensive as possible given present exposures. Most samples containing plagioclase megacrysts (Table 2) are from the Lower Selenga Plutonic Complex (LSPC) (Fig. 1b) or nearby; this complex is located 50 km to the south of the city of Ulan-Ude. The LSPC is a 50 km × 50 km representative area, exposing plutonic and volcanic rocks from Ordovician–Silurian to Cretaceous age. In the LSPC area granitoids of all ages make up 90% of the territory, with no sedimentary or metasedimentary rocks present. The only Ordovician–Silurian mafic rock localities occur in the Nesterikha and Romanovka plutons, 100 km north of the LSPC, and some Permian, Jurassic, and Cretaceous and younger volcanic mafic rocks are from the Dzhida river area, 100 km to the south-west of the LSPC. For Jurassic and Cretaceous basaltic suites we sampled only the most representative, previously studied outcrops, which contain plagioclase megacrysts (Kononova *et al.*, 1993).

Mafic rock samples with homogeneous megacrysts come from small gabbro stocks, synplutonic and composite dikes, and lava flows. We collected macroscopically fresh and unhybridized samples and studied them petrographically. Approximately one-third showed various degrees of subsolidus hydrothermal alteration, which also affected plagioclase megacrysts, and these were discarded. The purpose of further examination was to identify mafic rocks with large (1–3 mm) plagioclase megacrysts. Not all mafic rocks contain megacrysts.

ANALYTICAL PROCEDURES

Methods and analytical techniques

Samples were first studied optically and then with secondary and back-scattered electron imaging on a JEOL JSM-5800LV scanning electron microscope at the University of Chicago. Wavelength-dispersive analyses were made on a Cameca SX-50 electron microprobe using an accelerating voltage of 15 kV. Standards of Amelia albite and synthetic anorthite glass, and other synthetic minerals were used for major element calibration. Samples which were imaged by scanning electron microscopy (SEM) and analyzed by electron microprobe were analyzed later on the same spot by ion microprobe. We normally analyzed at least two spots on each crystal. Ion microprobe analyses were made using a modified AEI IM-20 instrument at the University of Chicago for concentrations of Li, Be, B, F, Mg, P, Cl, K, Ti, Fe, Co, Rb, Sr, Y, Zr, Nb, Cs, Ba, La, Ce, Pr, Nd, Sm, Eu, and Pb. Detailed analytical procedures and a full list of analyses with descriptions have been given by Bindeman (1998) and Bindeman *et al.* (1998). Molecular interferences were reduced by energy-filtering. For each spot, six cycles through the mass peaks were made, so that we could monitor whether the primary beam sputtered into a glass or mineral inclusion during analysis of plagioclase. Synthetic glasses doped with trace element were used as standards. They were analyzed twice a day to monitor ion yield variations. Diameter of the ion beam was typically 10 μm.

To allow oxygen isotope analyses, feldspar, amphibole, quartz, and biotite were separated by hand picking from ultrasonically cleaned grain aggregates of all major rock types. All quartz separates were further purified from any residual feldspars by treating them with warm fluoroboric acid. Oxygen was extracted from minerals and whole-rock powders using the conventional fluorination technique described by Wickham *et al.* (1995). After conversion of O_2 to CO_2, oxygen isotopic analysis was performed using a Delta-E mass spectrometer. Oxygen yields in the 95–100% range were considered successful. Results are reported in the δ notation relative to V-SMOW with NBS 28 quartz as a standard with $\delta^{18}O = +9{\cdot}6‰$. Calculated error associated with isotope analyses did not exceed 0·2‰.

Whole-rock major and trace elements were analysed by X-ray fluorescence (XRF) at XRAL Laboratories Co., Ontario, Canada.

Plagioclase megacryst selection procedure

The aim was to identify large (>1 mm), Ca-rich homogeneous crystal cores inside larger crystals. To accomplish this we went through a series of steps (Fig. 2). Polished thin sections of 256 fresh porphyritic mafic rocks were studied under the microscope. We selected 72 thin sections containing large phenocrysts with optically unzoned cores (e.g. Fig. 3). We examined and photographed them further by SEM using Z-contrast image in back-scattered electrons. Next we made electron microprobe profiles through 91 selected megacrysts (e.g. Fig. 3). Only 67 crystals with unzoned Ca-rich cores with respect to major elements were analyzed further with the ion microprobe. Five to 20 phenocrysts were normally studied by the electron microprobe from each thin section. Several of the best phenocrysts (91 altogether) from each rock with a Ca-rich 'plateau' on the concentration–distance plots were then analyzed by ion microprobe (e.g. Fig. 4). Trace element profiles through the most representative crystals of each age group were produced and aimed at showing a 'plateau value' for trace elements. A compositional plateau was taken to indicate that the unzoned cores have retained their trace elements (Fig. 4). Each sample was typically characterized by three crystals, and each core by two analyses. Analyses of all analyzed cores and the averages for each core are given in Appendix B of Bindeman (1998).

Partition coefficients were used to convert trace element concentrations to the parental basaltic values. Partition

Table 2: Samples of mafic rocks chosen and analysed by ion microprobe

Sample no.	Age (Ma)	Volcanic (V) or plutonic (P)	Occurrence	No. of crystals	Plagioclase sizes (mm)	Anorthite % in cores	Mineralogy	Locality
M106-7	OS (450)	P	SD	1	4–5	$An_{67–52}$	Pl, Cpx, Am, Bi	Nesterikha pluton
M131	OS (450)	P	SD	3	1–2	$An_{60–50}$	Pl, Am, Bi	Romanovka pluton
M132	OS (450)	P	SD	5	2–3	$An_{57–55}$	Pl, Am, Bi	Romanovka pluton
SH17	D (375)	P	CE	6	4–8	$An_{84–75}$	Pl, Am, Bi	Shaluta pluton
B718	D (375)	P	GS	2	2–3	$An_{60–55}$	Pl, Am	Shaluta pluton
Centi	D (375)	P	CD	1	2	$An_{64–62}$	Pl, Am, Bi	Shaluta pluton
9i	D (375)	P	CD	3	2	$An_{61–59}$	Pl, Am, Bi	Shaluta pluton
K86	EP (275)	P	SD	3	2–3	$An_{62–58}$	Pl, Am, Bi	Kuitunka pluton
B713c	EP (275)	P	CD	2	3–6	$An_{61–60}$	Pl, Am, Bi	Zhirim pluton
M139-10	EP (275)	P	CD	1	2	$An_{60–59}$	Pl, Cpx, Am, Bi	Ust-Khilok pluton
M139-7	EP (275)	P	CD	3	2	$An_{63–59}$	Pl, Cpx, Am, Bi	Ust-Khilok pluton
94-15a	EP (275)	V	LF	1	2	$An_{57–47}$	Ol, Pl	Unkurgui suite
94-51	EP (275)	V	LF	1	2	$An_{63–55}$	Ol, Pl	Unkurgui suite
B163-11a	LP (250)	P	CD	2	1–2	$An_{62–58}$	Pl, Am, Bi	Kharitonovo pluton
KH-2	LP (250)	P	CD	1	1–2	$An_{63–55}$	Pl, Am, Bi	Kharitonovo pluton
K57-12	LP (250)	P	CD	2	2	$An_{65–59}$	Pl, Am, Bi	Kharitonovo pluton
K57-14	LP (250)	P	CD	3	2	$An_{64–59}$	Pl, Am, Bi	Kharitonovo pluton
K57-6	LP (250)	P	CD	1	2	$An_{65–59}$	Pl, Am, Bi	Kharitonovo pluton
B446	LP (250)	V	LF	1	1	$An_{63–55}$	Ol, Pl	Tsagan-Khurtei suite
B448	LP (250)	V	LF	1	1–2	$An_{65–51}$	Ol, Pl	Tsagan-Khurtei suite
B450	LP (250)	V	LF	1	1–2	$An_{57–54}$	Ol, Cpx, Pl	Tsagan-Khurtei suite
1199	J3 (150)	V	LF	6	2–3	$An_{62–55}$	Ol, Cpx, Pl	Ichetui suite
1192	J3 (150)	V	LF	3	2–3	$An_{64–54}$	Ol, Cpx, Pl	Ichetui suite
1173A	K1 (100)	V	LF	2	2–3	$An_{61–53}$	Ol, Cpx, Pl	Dzhida
1173B	K1 (100)	V	LF	3	2–3	$An_{55–48}$	Ol, Cpx, Pl	Dzhida
1172	K1 (100)	V	LF	1	2–3	$An_{60–50}$	Ol, Cpx, Pl	Dzhida
1120	K1 (100)	V	LF	2	2–3	$An_{62–53}$	Ol, Cpx, Pl	Dzhida

CD, composite dike; SD, synplutonic dike; LF, lava flow; CE, coeval enclave in a pluton; GS, gabbro stock; Ol, olivine; Pl, plagioclase; Cpx, clinopyroxene; Am, amphibole; Bi, biotite; KFsp, potassium feldspar; An, anorthite content of cores in plagioclase phenocrysts.

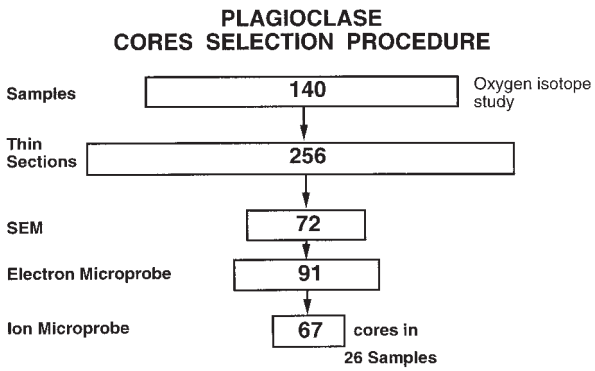

Fig. 2. Plagioclase megacryst selection procedure.

coefficients were determined using the same University of Chicago ion microprobe, for the same list of trace elements and using the same procedures as for analyzing Transbaikalian cores (see Bindeman *et al.*, 1998). The other advantage of used partition coefficients for the present study is a broad compositional range of plagioclase ($An_{79–39}$), which overlaps with the range of Transbaikalian plagioclases. The relationship between D_i and X_{An} allows an important correction to D_i values depending on plagioclase composition.

PETROLOGICAL RESULTS

Petrology of mafic rocks and plagioclase megacrysts

Mafic rocks come from both plutonic and volcanic facies (Table 2). Microscopically, all plutonic mafic rocks of different ages are petrographically similar, showing tabular or elongated plagioclase phenocrysts in a matrix of xenomorphic amphibole, plagioclase, biotite and magnetite.

Plagioclase megacrysts with plateau-type cores are often found in chilled margins of coeval mafic bodies, rather than in the less hybridized interiors of these bodies. Plagioclase from chilled margins is encapsulated by the rim and fine-grained groundmass, which mechanically isolated the megacryst and minimized diffusive exchange with the progressively hybridizing melt. In the interiors of the same bodies, plagioclase cores show evidence of resorption, probably because of longer cooling history and more intensive subsolidus alteration.

The majority of plagioclase megacryst cores of all ages have similar ranges of anorthite content ($An_{60–50}$) and sizes (2–3 mm) (Table 2; Fig. 3). They are euhedral and texturally appear phenocrystic rather than xenocrystic. The $An_{60–50}$ composition is typical for liquidus plagioclase in alkali basalts (e.g. Smith & Brown, 1988). Pleistocene and Holocene plagioclase phenocrysts in high Mg–Ni–Cr, high Mg-olivine phenocrysts and mantle-nodule-bearing (and assumed undifferentiated) Baikal-rift alkali basalts, are also $An_{60–50}$ (Sharkov & Bindeman, 1990). This supports our assumption that $An_{60–50}$ plagioclase in older volcanic and plutonic suites (Table 2) is a primary liquidus phase. The presence of a few more calcium-rich plagioclase crystals in Devonian and Ordovician–Silurian suites may reflect their calc-alkaline affinity (see below).

Comagmatic volcanic and subvolcanic bodies have plagioclase phenocrysts of similar size and composition to their plutonic counterparts. Other phenocrysts include euhedral, often altered Mg-rich (Fo_{85}) olivine and occasional clinopyroxene. Groundmass in most cases is a result of recrystallization and alteration of glass. It is possible to compare plagioclase phenocrysts in volcanic and plutonic facies of Early Permian and Late Permian suites (Table 2). We find that both volcanic and plutonic phenocrysts of the same age have the same core composition, size and morphology, and their trace element concentrations overlap (see below). The compositional overlap suggests that plagioclase crystallized from similar magmas under similar conditions before magmas became plutonic or volcanic rocks. The primary plagioclase cores seem insensitive to level of emplacement (volcanic or plutonic) and subsequent cooling and crystallization.

Whole-rock chemistry

Most silicic and mafic rocks reported in this work were analyzed for major and trace elements (see, e.g. Kononova *et al.*, 1993; Litvinovsky *et al.*, 1994; Bindeman, 1998; Litvinovsky & Zanvilevich, 1998). Litvinovsky & Zanvilevich (1998) compiled a comprehensive dataset of major and trace element analyses of Transbaikalian silicic and mafic rocks of different ages. They made an attempt to identify the least hybridized mafic rocks in each suite to be used as geochemical tracers for tectonic evolution. Mafic rocks that contain plagioclase megacrysts and were considered in this study are not necessarily the least hybridized and least fractionated rocks in each outcrop. However, they almost always belong to the magma body where the less hybridized mafic rocks are found. For example, hybridized chilled margins that contain plagioclase megacrysts often bear evidence of post-quench hybridization. The bulk composition of these chilled margins reflects *in situ* hybridization, whereas plagioclase megacrysts in them preserve their original composition.

The concentration of MgO in most samples which contain plagioclase megacrysts is >4·5 wt %, and the concentration of SiO_2 is <54 wt %. In some of the Devonian samples, the high SiO_2 is an artifact, because unzoned calcic plagioclase comes from rather hybridized chilled margins and enclaves (Bindeman, 1998). Least hybridized mafic rocks of each outcrop (pluton) where

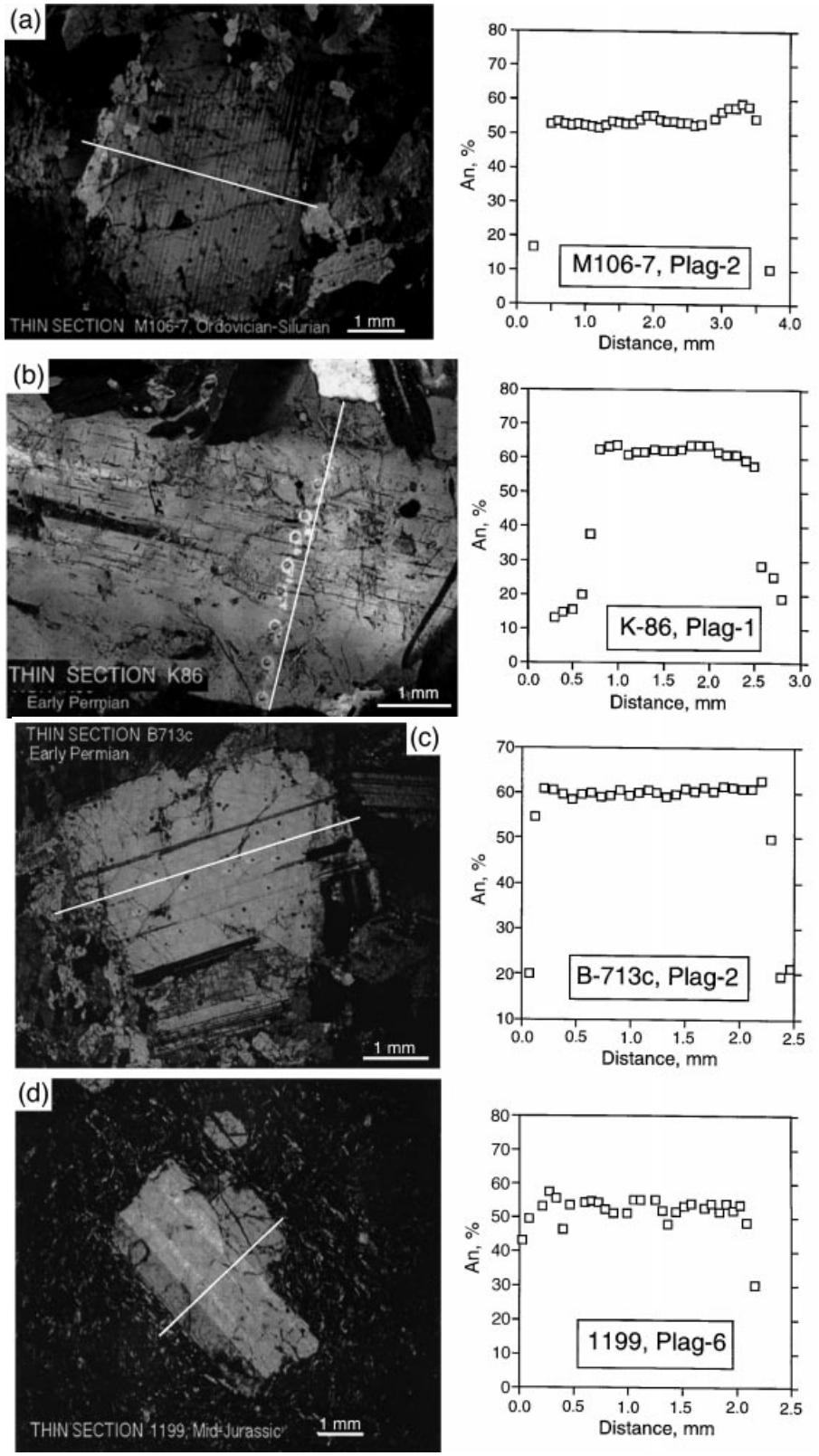

Fig. 3. Transmitted light photomicrographs of plagioclase megacrysts in plutonic (a–c) and volcanic rocks (d); sample descriptions are given in Table 2; oval holes are result of ion microprobe analysis; lines denote the location of the electron microprobe profile.

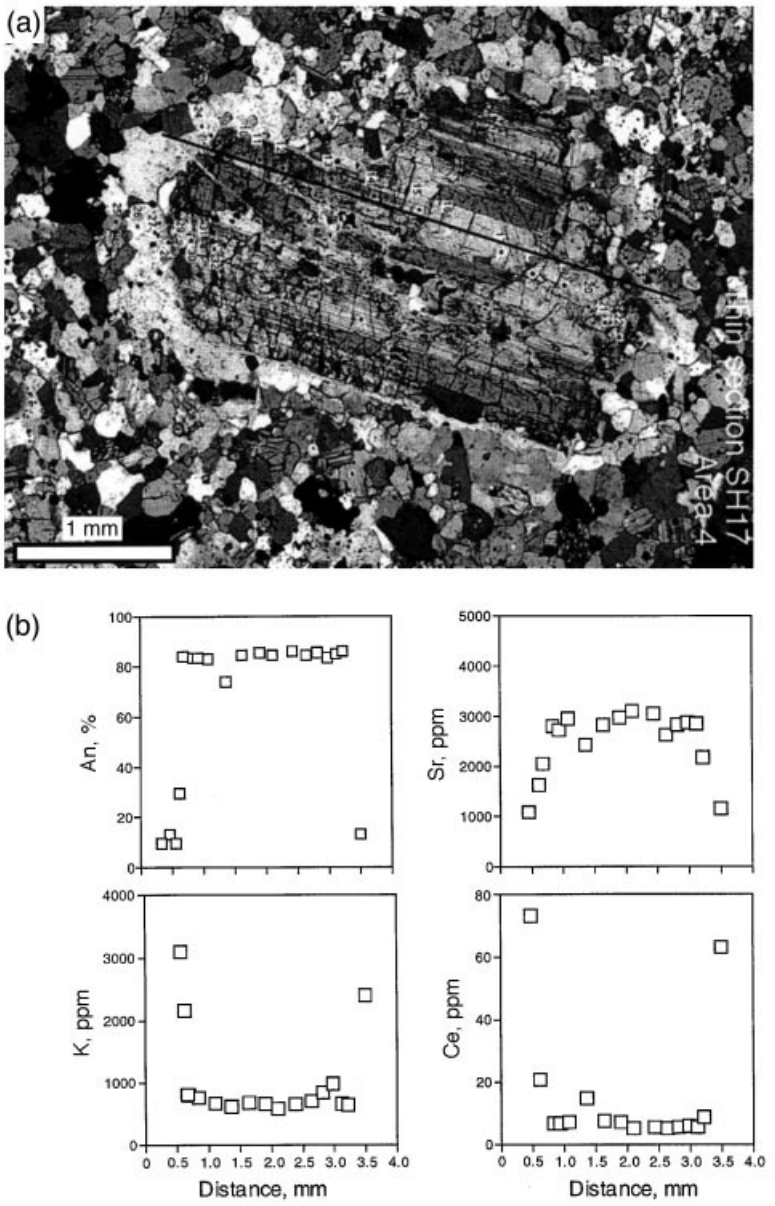

Fig. 4. Ion microprobe profile through the plagioclase megacryst in the 20 cm mafic enclave in syenites of Devonian Shaluta pluton (sample Sh17). It should be noted that the 'plateau' value on the concentration–distance plot is preserved for minor and trace elements.

plagioporphyritic rocks are found often contain <54 wt % of SiO_2 and >5–7 wt % MgO (Litvinovsky & Zanvilevich, 1998). Some of them are nepheline normative. Normative nepheline arises in some samples of the earliest Ordovician–Silurian suite, and many Mesozoic and Cenozoic volcanics are nepheline normative (Sharkov & Bindeman, 1990; Kononova *et al.*, 1993).

Oxygen isotope study

The purpose of our oxygen isotope project was threefold: (1) we wanted to ensure that none of the studied samples has abnormally low $\delta^{18}O$; (2) we wanted to ensure that the fractionation factor, Δ, between plagioclase and amphibole, and between plagioclase and whole rock in a rock is small (1–2·5‰), suitable for high-temperature (magmatic) oxygen isotope equilibrium between minerals; (3) we wanted to estimate the magmatic $\delta^{18}O$ values of rocks from each suite. The $\delta^{18}O$ values of mafic rocks of each age group are related to contamination of the mafic rocks by the crust.

Representative least altered samples of each age group were analyzed for oxygen isotopes. We analyzed whole-

rock powders, plagioclase, amphibole, and biotite mineral separates from several samples of each suite (Table 3).

Some Transbaikalian silicic and mafic rocks (not part of this study) have suffered exchange with meteoric water (Wickham *et al.*, 1996; Bindeman, 1998). The exchange and alteration resulted in 5–15‰ of $\delta^{18}O$ fractionation between quartz and feldspar (which have different susceptibility to alteration; plagioclase, in particular, was shown to be the easiest mineral to alter; e.g. Criss & Taylor, 1986). The preservation of magmatic $\delta^{18}O_{Pl}$ serves as an additional test of the survival of plagioclase cores. Table 3 reveals that no such disequilibria are present among our samples of each age group, which gives us confidence that the studied $\delta^{18}O$ values are close to primary magmatic values. All reported data in Table 3 come from outcrops for which oxygen isotopes were studied extensively (Wickham *et al.*, 1995, 1996). Not only are plagioclase–amphibole and plagioclase–whole-rock data for mafic rocks in a high-temperature range, but also their nearby coeval silicic rocks have been analyzed on quartz–plagioclase pairs, and showed no evidence of hydrothermal involvement.

Figure 5 demonstrates that the whole-rock and plagioclase $\delta^{18}O$ values decrease with decreasing age. Whole-rock $\delta^{18}O$ values change from 8·7‰ in the earliest Ordovician–Silurian suite to <6‰ in all suites since the Mesozoic. Pokrovsky (1991) reported 4·6–6‰ $\delta^{18}O$ values in Quaternary Baikal rift lavas and their phenocrysts. Plagioclase that is separated and cleaned from groundmass exhibits an even more pronounced and less noisy decreasing trend from 9·1‰ to ~6‰. The least hybridized samples of each age group (see Table 4 and Fig. 5) exhibit a similar magnitude of $\delta^{18}O$ decrease with age. Hybridism observed in studied outcrops increases $\delta^{18}O$ only locally (e.g. Bindeman, 1998) and does not change the $\delta^{18}O$ of the interior of large basic magma bodies.

Given the SiO_2, MgO and K_2O concentrations in mafic rocks and their $\delta^{18}O$ values, assimilation–fractional crystallization (AFC) modeling below does not allow the increase of more than at most 1·5–2‰ as a result of contamination by the $\delta^{18}O$-richer coeval silicic rocks or their magmas. The $\delta^{18}O$ values of the rocks correlate neither with the SiO_2 content, nor with other AFC-sensitive variables such as K_2O, MgO, Co contents, or Mg/Fe ratio. We speculate that at least 1–1·5‰ of the observed 3‰ decrease reflects a decrease in $\delta^{18}O$ of the parental, primitive basaltic magmas. If this is the case, it probably reflects the $\delta^{18}O$ evolution of the source for basaltic magma.

Crystallization and AFC modeling

The possible extent of crustal contamination that the studied samples could have experienced may be estimated by using the whole-rock $\delta^{18}O$ data and concentrations of elements that are sensitive to assimilation. We considered the earliest Ordovician–Silurian suite, where there is a large $\delta^{18}O$ contrast between silicic and mafic rocks (Wickham *et al.*, 1996). The range in $\delta^{18}O$ among even the least hybridized mafic rocks ranges from +7 to +8·5‰. This is in the uppermost range of variations detected in intracontinental basalts (Kyser, 1986, 1993; Harmon & Hoefs, 1995). Contamination of the mafic rocks with $\delta^{18}O$-rich crustal rocks and/or origin of basic magma from $\delta^{18}O$-rich source could be suspected.

The *relative change* in $\delta^{18}O$ and the bulk major element composition of the basic magma was calculated by the direct small-step assimilant addition–cumulate removal calculation to monitor the remaining $\delta^{18}O$ of the magma for varying proportions of R (the ratio of cumulate to assimilant) and the degree of fractionation, f. If $R > 1$ the mass of the magma decreases with time; if $R = 1$ it remains constant, and for the less likely case where $R < 1$, the size of the magma body increases with time.

We considered concentrations of K_2O, SiO_2, MgO and $\delta^{18}O$, because these are the most sensitive to fractionation or assimilation (Fig. 6), K_2O being relatively insensitive to fractionation, and MgO to assimilation. There is no clear correlation between MgO and $\delta^{18}O$ in the 4·5% < MgO < 9% range. No correlation exists for K_2O in mafic rocks vs $\delta^{18}O$, and there is even an anticorrelation between SiO_2 and $\delta^{18}O$ in the basaltic range. Moreover, the existence of MgO-rich, SiO_2-poor samples that have $\delta^{18}O \sim 8‰$ is peculiar. The best fit of data assumes a basaltic magma with $SiO_2 = 48\%$, MgO = 9%, $K_2O = 1{\cdot}5\%$, $\delta^{18}O = 7$–7·5‰ and AFC parameters include $R = 1$–2, $\beta_{SiO_2} = 0{\cdot}9$, $\beta_{MgO} = 2$, and $\beta_{K_2O} = 0{\cdot}1$ (e.g. Wilson, 1989).

Therefore, the scatter of points in Fig. 6 is most consistent with the model in which the original SiO_2-poor, MgO- and $\delta^{18}O$-rich basaltic magma fractionated in the first stage without significant assimilation. If the described values are employed, the natural mafic rocks may contain up to 20 wt % of the granitic assimilant. Similar modeling was done for younger suites. In all cases the mafic rocks could have suffered a maximum of 10–20% of crustal assimilation.

How a maximum 20% of crustal contamination will affect the trace element concentrations of the magma depends on the ratio of the various elements in basic and silicic end member magmas. Figure 7 provides an example of the element ratios in coeval silicic to mafic rocks for the same Ordovician–Silurian suite samples. Most of the trace element concentrations in the mafic rocks are within a factor of three of those in coeval silicic rocks. Potassium shows the most contrasting distribution ($K_2O_{(silicic)}/K_2O_{(mafic)} = 3{\cdot}7$–4·5) and should be most sensitive to contamination with the high-K continental crust. For 20% of crustal contamination, K will increase by a

Table 3: Oxygen isotope analyses of Transbaikalian mafic–intermediate rocks of different ages

Sample no.	Age (Ma)	SiO_2	MgO	$\delta^{18}O$ (‰) WR	Fsp	Amph	Bi	Rock	Locality
B127-2*	OS	47·66	5·27	8·85				SD	Nesterikha
M106-5*	OS	49·54	6·81	8·31				SD	Nesterikha
B133-2*	OS	51·08	5·32	8·41				SD	Romanovka
TB-16*	OS	50	9·34	7·83	8·84	7·81		GS	Barguzin
TB-19	OS		8·47		9·23			GS	Barguzin
TB-14	OS	53·1	5·14	7·78	8·83			GS	Barguzin
TB-15	OS	51	5·6	7·71	8·52	7·35		GS	Barguzin
AV7	OS			7·72	8·61			CD	Barguzin
AV6	OS	55·2	4·79	7·73				CD	Barguzin
AV5	OS			7·76				CD	Barguzin
AV4	OS			7·4				CD	Barguzin
2A	D	55·6	4·04	7·57	8·45			GS	Shaluta
6A	D	55·5	4·23	6·97	7·14	6·55		GS	Shaluta
10	D	56·2	4·24	7·96	8·48	6·83		GS	Shaluta
34-2	D	54·6	4·21	7·91				GS	Shaluta
37-1*	D	52·2	6·52	6·52				GS	Shaluta
47	D	54·5	4·67	6·97				GS	Shaluta
SH18C	D	54	8·55	6·89	8·24	6·88	6·05	CD	Shaluta
SH21-D*	D	51·2	7·19	6·93	8·33		5·52	GS	Shaluta
SH10	D	53·9	4·33	8·24	8·19	6·1		CD	Shaluta
SH16C	D			5·65				CD	Shaluta
SH11C	D	53·9	3·33	7·93				CD	Shaluta
SH11D	D	54·3	3·4	7·65				CD	Shaluta
1i	D	58·9	2·37	8·53	8·49			CD	Shaluta
5i	D	59·8	2·13	8·56	9·1			CD	Shaluta
SH17	D	56·2	3·01	6·39	7·88	6·05		CE	Shaluta
K86*	EP	54·4	5·41	7·8	8·73			SD	Kuitunka
K86a*	EP	54·4	5·41		8·77			SD	Kuitunka
A368	EP			5·4				CD	Ust-Khilok
A368-1	EP			5·88				CD	Ust-Khilok
M139-10*	EP	47·8	5·9	6·23	7·75			CD	Ust-Khilok
B713c	EP			6·88	7·65			CD	Zhirim
KH3*	LP	48·5	5·18	7·36				CD	Kharitonovo
KH3	LP	48·5	5·18	7·5	8·26	6·65		CD	Kharitonovo
KH8*	LP	50	5·2	5·79				CD	Kharitonovo
KH2-1*	LP	51·9	5·62	6·91				CD	Kharitonovo
KH2-2	LP			7·61	7·45			CD	Kharitonovo
KH2-3	LP		6·78					CD	Kharitonovo
1199	J3	50·29	3·88		5·43			LF	Dzhida
1192*	J3	48·95	4·03		6·03			LF	Dzhida
1190*	J3	48·9	54·45		6·08			LF	Dzhida
1173*	K1	49·34	6·12		6·01			LF	Dzhida
1172*	K1	49·22	6·14		5·63			LF	Dzhida

*Least hybridized samples; see Table 2 for sample description and abbreviations, whole-rock analyses are in table 4.3 of Bindeman (1998).

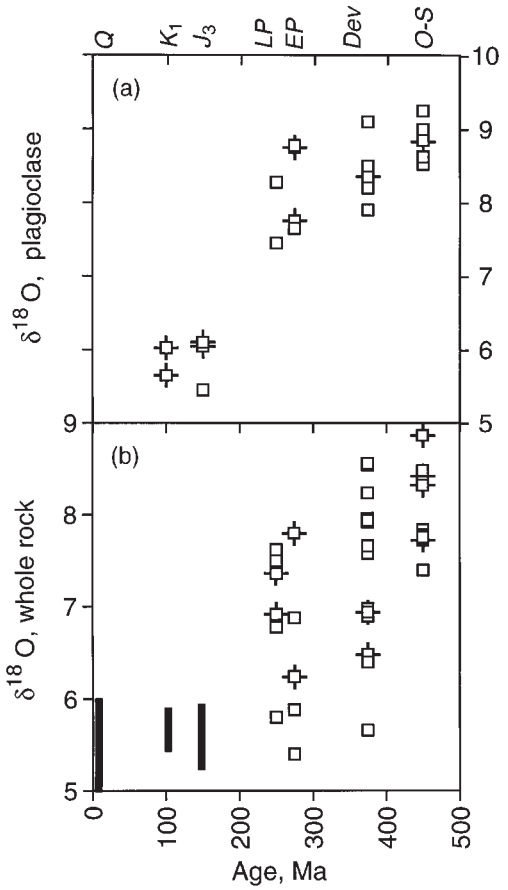

Fig. 5. The evolution of $\delta^{18}O$ from the Ordovician–Silurian to the Recent. (a) Plagioclase $\delta^{18}O$ values; (b) whole-rock $\delta^{18}O$ values. Squares with plus signs denote the least hybridized samples of each age group. Ranges of whole-rock $\delta^{18}O$ data for Cretaceous and Jurassic suites were calculated from the $\delta^{18}O$ of plagioclase, assuming +0·2‰ fractionation factor between plagioclase and basalt (e.g. Kyser, 1986). $\delta^{18}O$ range from the Recent is from Pokrovsky (1991). (See Table 3 for analyses and text for discussion.)

factor of two in the whole rock. Caution should be used in interpreting the whole-rock trace elemental data. The use of plagioclase megacrysts within these mafic rocks serves as a better approach to retrieve the more primitive magma composition.

'Looking through' the effects of assimilation and fractionation

Pure fractionation of basic magma will proportionately and indiscriminately increase the concentrations of almost all trace elements, except elements that are compatible with earliest olivine, spinel and pyroxene-dominated cumulates (e.g. Ni, Cr, Mg, Co, etc.). It will not, therefore, change the trace elemental signature of incompatible trace elements.

The maximum amount of crustal contamination of mafic rocks is 20%, on the basis of the whole-rock major element and $\delta^{18}O$ composition. In this section we try to show how the trace elemental composition of the primary cores in plagioclase megacrysts inside these mafic rocks can also constrain this amount of AFC, thus allowing recovery of some or most of these effects and bringing us much closer to the primary, mantle-equilibrated compositions.

To demonstrate that plagioclase cores 'see back through' the effects of plutonic fractionation and assimilation we use concentrations of K_2O, Ba, Sr and Rb in plagioclase cores for which XRF whole-rock analyses exist (see Bindeman, 1998). K_2O, Ba and Sr are abundant in plagioclase, and partition coefficients are well constrained for these elements. Furthermore, because of the contrasting distribution of K_2O, Ba, Sr and Rb between mafic and silicic rocks in Transbaikalia (e.g. Fig. 7), change in their concentrations is a sensitive indicator of assimilation.

We applied partition coefficients to trace element concentrations in each core in the sample to reconstruct a parental magma composition. Reconstructed magma compositions are compared with the observed whole-rock concentrations for both the host rock and other rocks from the same outcrop (see Bindeman, 1998). Figure 8 demonstrates that the reconstructed compositions are indeed more primitive than the whole-rock compositions for most samples. Because the result is consistent for all elements, it indicates that it is likely to be a true recovered signal and not an artifact of partition coefficients. Also, the compositional scatter for reconstructed and observed whole-rock compositions is comparable and reflects both analytical and natural uncertainties. Therefore, the reconstructed compositions for well-determined trace elements are at least as secure as whole-rock compositions.

Quantification of degree of assimilation and fractionation can now be reviewed using the example of K_2O, which shows the most contrasting distribution and should be the most sensitive to contamination. Potassium is a minor element whose concentrations are accurately determined, whose partition coefficients are most reliable, and which is sensitive to contamination with the high-K silicic rocks and magmas.

The reconstructed trace element concentrations in individual cores within one sample were averaged and compared with the higher whole-rock K_2O content for each sample (e.g. Fig. 8). Next, the higher K_2O content in the whole rock containing the plagioclase cores was attributed to either (or probably both) of two processes: (1) fractional crystallization of basaltic magma, leading to K_2O increase; (2) bulk assimilation of K_2O-rich silicic rock or magma (Fig. 9). If the whole increase in K_2O is attributed only to fractional crystallization, the estimated

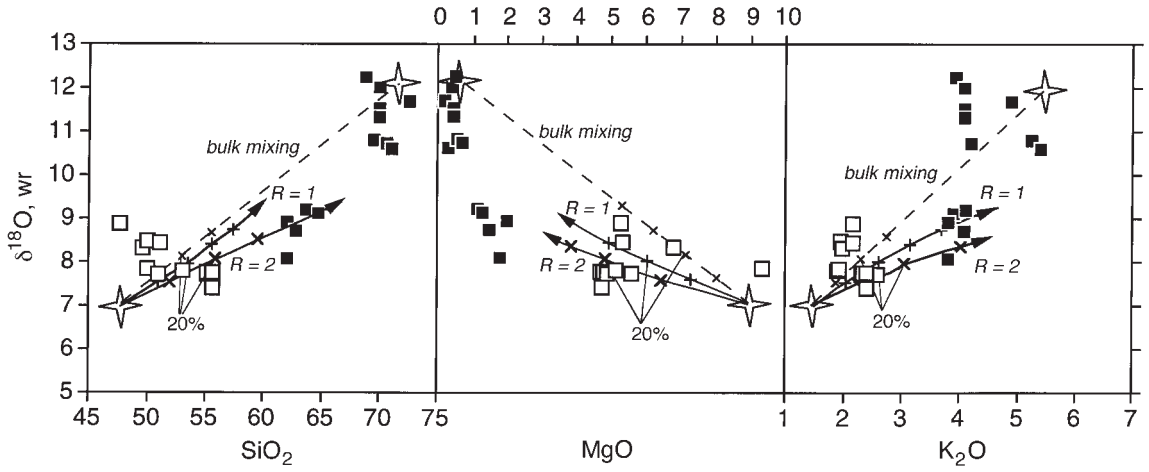

Fig. 6. The estimation of the possible degree of basic magma contamination of the Ordovician–Silurian mafic suite by the silicic crust. □, $\delta^{18}O$ vs SiO_2, MgO, and K_2O, of mafic rocks; ■, coeval silicic and hybrid rocks. $\delta^{18}O$ values in silicic and mafic rocks are from Table 3 and Wickham *et al.* (1996); major element concentrations are from Litvinovsky *et al.* (1994) and Bindeman (1998). Stars are accepted values for end-members: initial $\delta^{18}O$ of basic magma for the typical intracontinental basalt is from Harmon & Hoefs (1995), and the average Ordovician–Silurian crust is from Litvinovsky *et al.* (1994) and Wickham *et al.* (1996). Dashed line is a bulk mixing line; curved vectors are trajectories of assimilation during AFC; + and × , 10% increments of crustal assimilation in the remaining liquid at indicated values of R (rate of crystallization/rate of assimilation). For example, if $R = 1$ then 10% of crustal assimilation will correspond also to 10% of fractionation.

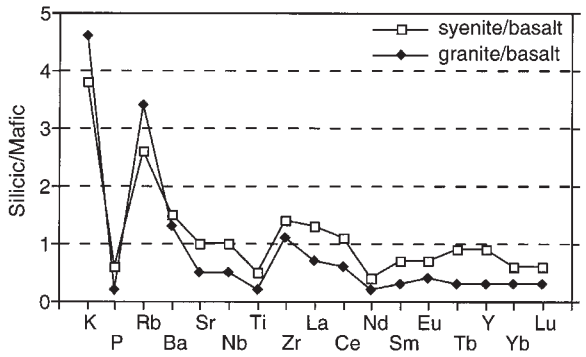

Fig. 7. Ratio of trace element concentrations in coeval silicic and mafic rocks of Ordovician–Silurian age. Analyses are from Bindeman (1998) and Litvinovsky & Zanvilevich (1998).

degree of fractionation elapsed after plagioclase core crystallization is below 45% but for most samples is below 25%. If the whole increase in K_2O is attributed only to assimilation of the coeval silicic rocks (with 4·5–6 wt % K_2O) without fractionation then the amount of assimilation is <30% and for most samples is <15%.

The most likely scenario would include assimilation and fractionation acting together and, depending on the proportions of cumulates to assimilant (normally larger than unity because of the heat capacity argument (e.g. DePaolo, 1981), splitting the proportion between assimilation and fractionation, hence putting the amount of assimilation to an even lower level.

Therefore, it is demonstrated here that the use of plagioclase cores allows us to step back some few tens of percent of assimilation and fractionation. Compared with the 10–20% of assimilation which plagioclase-bearing host rocks could have experienced (e.g. Fig. 6), the cores allow us to 'see' the magma before it evolved to its present state as a rock. Hence, the best estimate of the primitive magma composition is provided by the plagioclase cores.

TEMPORAL TRENDS

Evolution of plagioclase megacryst chemistry with time

The relatively narrow anorthite range of studied plagioclases ($An_{50–65}$ for 90% of the samples; see Table 2) implies that there are no drastic differences in partition coefficients for these plagioclases (Bindeman *et al.*, 1998). Therefore we may directly compare trace element concentrations in the plagioclase phenocryst cores (as proxies for magmatic values) with time.

Figure 10 shows the concentration of trace elements in plagioclase cores vs geological age. Each point in the diagram corresponds to the averaged trace element concentration in a single plagioclase core [given in Appendix B of Bindeman (1998)]. We indicated with different symbols volcanic and plutonic cores, and three of the most K_2O-poor cores of each age group, which are taken to mark the supposedly least evolved samples. In

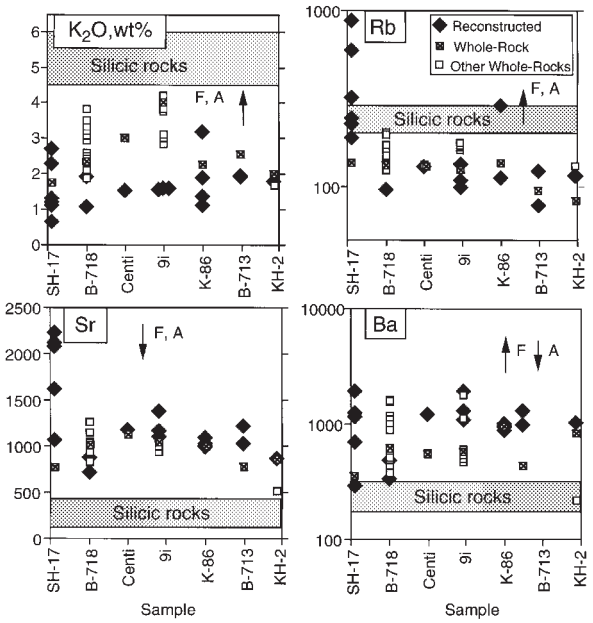

Fig. 8. Reconstructed concentrations of K_2O (wt %), Rb, Sr and Ba (ppm) based on trace element concentrations in plagioclase cores and partition coefficients [see Bindeman (1998) for analyses]. F and A arrows indicate the direction of concentration change in the melt during fractionation (F) and assimilation–mixing of silicic rocks (A), respectively. Each filled diamond represents a reconstructed concentration based on a single plagioclase core; each open square with the '×' symbol is a whole-rock concentration in a host rock containing the cores; other open squares are similar rocks belonging to the same outcrop. Silicic rocks taken as an assimilant are the same coeval magmas to the indicated mafic rock samples. All whole-rock analyses are from Bindeman (1998) and Litvinovsky & Zanvilevich (1998). It should be noted that most of reconstructed concentrations are more primitive than the whole rocks. A significant scatter of points characterizes highly hybridized samples from the Devonian Shaluta pluton (Samples Sh17 and B718), which experienced strong hybridization after plagioclase core crystallization (Bindeman, 1998). K_2O and Sr graphs are linear; Rb and Ba graphs are logarithmic.

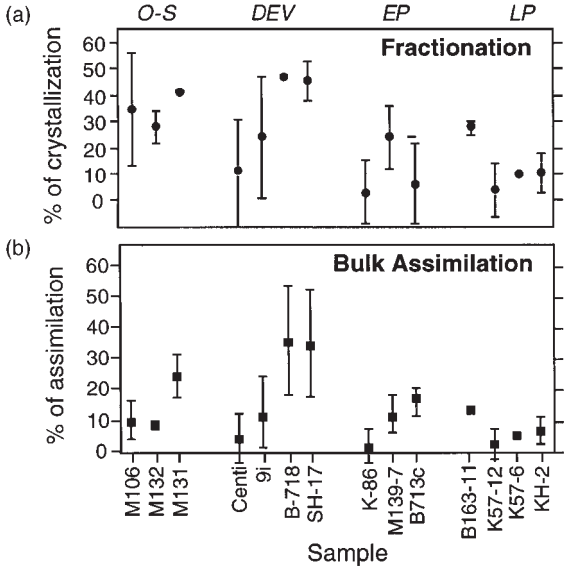

Fig. 9. K_2O-based recalculated degree of basic magma fractionation (a) and bulk assimilation with the coeval silicic rocks (b), following crystallization of plagioclase cores. The reconstructed K_2O concentrations are based on the trace element analyses of several plagioclase megacrysts in each sample, which were compared with the whole-rock K_2O concentrations in these samples. The difference was attributed either to (a) fractionation elapsed since plagioclase crystallization, or (b) assimilation of coeval silicic rocks. In the fractionation calculation potassium is taken as a fully incompatible element. For bulk mixing the fraction of silicic end-member is simply added to the reconstructed concentration to yield the whole-rock K_2O value.

addition, all plagioclase cores less calcic than An_{45} were excluded from plotting. Despite variation among samples of each age, the variations between age suites for many elements are larger and temporal trends are clear.

K, Rb, Cs

Concentrations of K monotonically increase with decreasing age. The plagioclases from the youngest suites are 5–6 times richer in K than those in the earliest suites. This result is opposed to the result expected from crustal contamination. If crustal contamination were playing a major role in K budget of basic magma (before plagioclase crystallization), then the oldest plutonic suites would have more chance to be heavily contaminated with their coeval high-K silicic counterparts. The youngest olivine-bearing volcanic rocks of the last two suites would have been more pristine. Because we observe just the opposite, the trend indicates that the K concentrations in plagioclases largely reflect primary basic magma features, rather than the impact of crustal contamination. Thus the trends in other trace elements in the same cores are related to the evolution of the initial differences (or absence of such) in their parental basic magmas.

The concentrations of other alkali LILE—Rb and especially Cs—in plagioclase are determined with less precision on the ion microprobe. Rb shows a highly scattered decreasing trend since Devonian, and the temporal trend of Cs is lost within the scatter. As a result of K increase, the K/Rb and K/Cs ratios increase.

Ti, P, Zr and Nb

The concentrations of HFSE increase with decreasing age. The concentration of Ti increases 8–10 times whereas P shows scattered increase. These elements are virtually immune to crustal contamination, because silicic rocks contain relatively low concentrations of titanium and phosphorus. The established trend is interpreted as reflecting primary features of basic magma and its temporal evolution.

The concentrations of Nb, which has a low abundance in plagioclase trace HFSE, increase in suites 5 and 6,

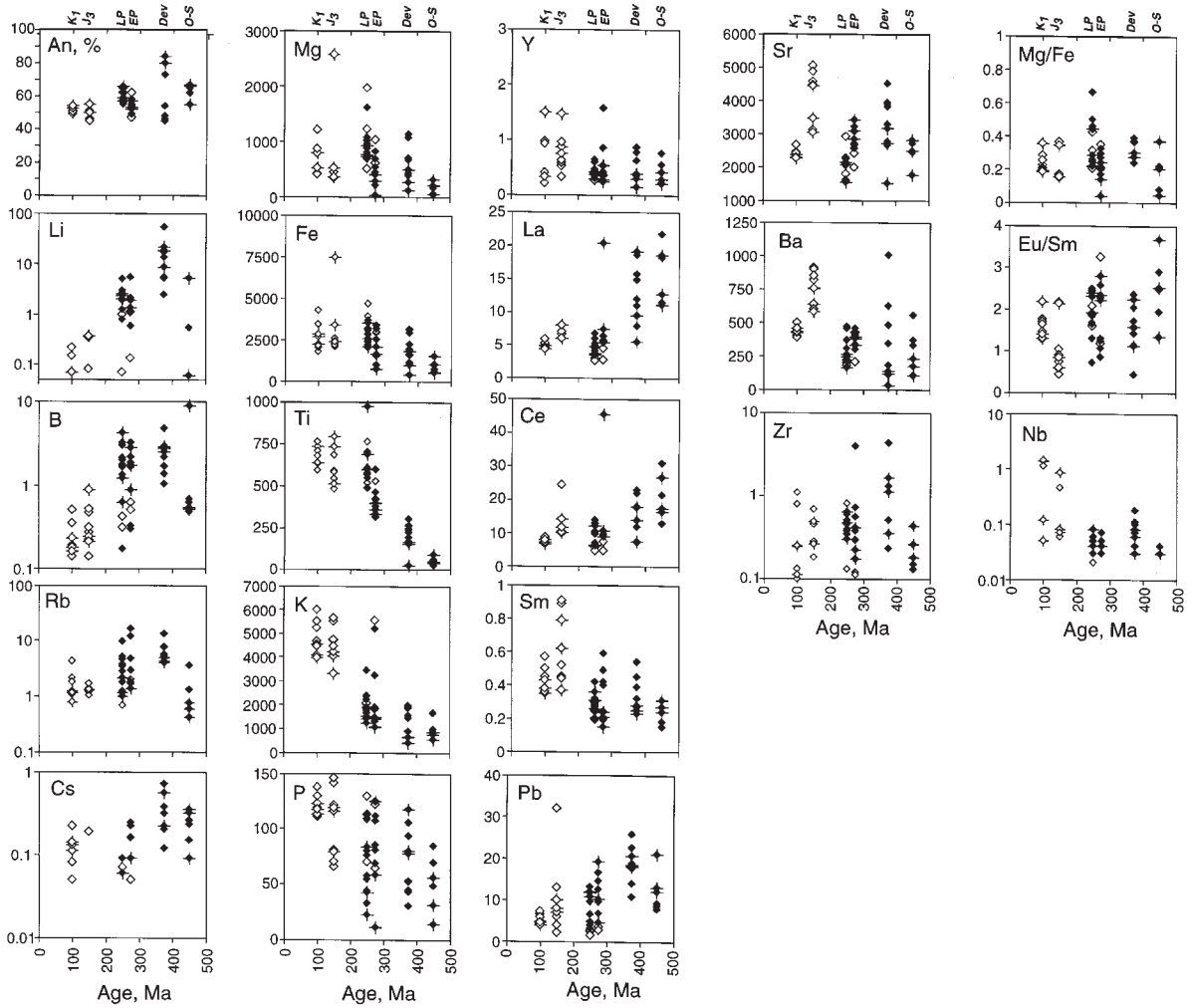

Fig. 10. Trace elemental concentrations and ratios in cores of plagioclase megacrysts [see Bindeman (1998) for analyses]. Only plagioclase cores with An % > 45 are plotted. Filled diamonds are plutonic cores; open diamonds are volcanic cores [significantly, volcanic and plutonic cores are similar in both Early Permian (EP) and Late Permian (LP) suites]; crosses denote three samples in each age group with the lowest reconstructed K_2O content, taken as the evidence of the most primitive (unhybridized and undifferentiated). It should be noted that this selection does not show a similar pattern on similarly incompatible elements. This is taken as evidence that the scatter in each age group is not due to contamination or fractionation. It is interpreted to be related to the initial magma composition. It should be noted that some graphs are logarithmic.

whereas Zr scatters significantly and shows no clear trend.

Mg, Fe and Mg/Fe

The concentrations of Mg and total Fe increase with decreasing age, whereas the Mg/Fe ratio remains relatively constant. The low absolute value of Mg/Fe^{total} in plagioclase is expected, because Fe^{3+} partitions into plagioclase 10 times more efficiently than Fe^{2+} (Phinney, 1992). The relative constancy of differentiation-sensitive factors such as Mg/Fe ratio in plagioclases of different ages is interpreted as reflecting the similar degrees of basic magma fractionation (or absence of such) before plagioclase has started to crystallize.

Li, B and Pb

The concentrations of these geochemically distinct elements exhibit similar patterns. The concentrations increase from Ordovician–Silurian to Devonian suites and then show steady decrease with decreasing age, with significant scatter. Lead also shows an overall decrease from the Devonian suite onwards and is interpreted as reflecting the evolution of the basic magma source. Remarkably, the evolution of lead concentrations in Transbaikalian plagioclases closely matches that of hydrophile Li and B. Lead, lithium and boron have been shown experimentally to preferentially partition into the fluid phase during subduction (Tatsumi *et al.*, 1986; Noll *et al.*, 1996; Kosigo *et al.*, 1997; Tatsumi & Kosigo, 1997).

REE and Y

Concentrations of La and Ce decrease with decreasing age, whereas the concentrations of Pr, Sm, Nd, Eu and Y remain constant or slightly increase. As a result, La/Y and Ce/Y ratios decrease with decreasing age. The relative constancy of Eu/Sm ratio in plagioclases of different ages is interpreted as reflecting the absence or similar degrees of pre-existing plagioclase fractionation before cores crystallized.

Sr and Ba

Strontium shows a zigzag pattern, which probably results from its strong sensitivity to fractionation. Ba shows no clear trend.

Reconstructed parental melt compositions and element ratios

The reconstructed trace element concentrations and ratios of the parental basaltic magma inferred from plagioclase cores can be compared with observed trace element concentrations and ratios in other basalts (whole rocks).

Reconstructed concentrations of trace elements (Fig. 11) were obtained by dividing concentrations in the cores of primary megacrysts by the corresponding partition coefficients. The latter were adjusted with respect to anorthite content in plagioclase and temperature (see Bindeman *et al.*, 1998) assuming a single temperature, 1150°C. Magmatic temperature variation within ~100°C produces a less than 10% effect on $RT\ln D_i$ value (see Blundy & Wood, 1991; Bindeman *et al.*, 1998), which is well within the natural and analytical dispersion.

K_2O

The reconstructed K_2O concentration in the parental magma changes from ~1 wt % in the earliest Ordovician–Silurian suite to 3–5 wt % in Jurassic and Cretaceous rocks. Rather high potassium concentration even in the earliest suites implies the K-rich calc-alkaline or alkaline nature of basic magmas.

TiO_2 and P_2O_5

Progressive increase in Ti and P concentrations in plagioclase cores from the earlier to later suites corresponds to increasing reconstructed TiO_2 and P_2O_5 concentration in their parental magmas. Low concentration of TiO_2 (0·16–0·48%) and P_2O_5 (0·10–0·20%) in the earliest suites suggests a calc-alkaline nature of Ordovician–Silurian and Devonian suites, despite rather high K_2O. Cretaceous and Jurassic suites have high concentrations of both TiO_2 (1·3–1·51%) and P_2O_5 (0·20–0·30%) corresponding to typical intraplate basalts (e.g. Pearce & Cann, 1973).

REE and Y

The reconstructed concentrations of REE for all suites are high, and consistent with that of common alkali basalt (e.g. Sun & McDonough, 1989). Reconstructed La and Ce decrease from the two earliest suites, whereas medium REE (MREE), and heavy REE (HREE) proxy element, Y, do not show any significant trend. As a result, the reconstructed La/Y and Ce/Y ratios are high for rocks of all ages, similar to those of deep-segregated intracontinental alkali basalts having garnet in their source (e.g. McKay, 1989) and differing from subduction-related magmas. Surprisingly enough, the earliest suites have the highest La/Y ratio, approaching 100. The decrease in the La/Y and Ce/Y ratios at only slight increase in Y indicates preferential temporal depletion of light REE (LREE). Tatsumi *et al.* (1986), Kosigo *et al.* (1997) and Tatsumi & Kosigo (1997) have shown that LREE are strongly enriched in the fluid phase separated from the subducted slab, whereas mobility of HREE and Y is negligible.

The reconstructed concentrations of trace elements were used to calculate element ratios, to reveal some source-related features of basic magmatism of each age (Fig. 10).

Ba/K vs Rb/K

The use of this diagram is meant to discriminate the island arc basalt (IAB) from ocean island basalts (OIB) and within-plate basalts (WPB) (Fig. 11). Cs, Rb and Ba were shown to be highly hydrophile during slab dehydration with saline fluids and they enrich the mantle wedge in the order Cs, Rb, Ba, K (e.g. Tatsumi, 1986; Keppler, 1996). On the other hand, these elements have similar incompatibility to melt during partial melting of variously enriched or depleted mantle (e.g. McDonough *et al.*, 1992), and Ba/K and Rb/K ratios are relatively insensitive to variations in degree of partial melting and crystallization. Therefore Rb/K and Ba/K ratios can be used to discern the arc signature in the old rocks.

We notice in the Ba/K vs Rb/K diagram that there is an overall temporal decreasing trend from the field of IAB toward the field of OIB–WPB in Transbaikalian suites.

Ti vs Zr, Ti/Y vs Nb/Y and Ti/La vs P/La diagrams

The other important test is the use of HFSE and their ratios to REE to discriminate OIB–WPB vs IAB. HFSE were shown to be retained with the accessory phase (such as sphene, rutile, etc.) within the downgoing subducting slab, leading to the depletion in Nb and Ti, and to a lesser degree P and Zr, in arc magmas (e.g. Johnson & Arculus, 1978; Hickey *et al.*, 1986; Keppler, 1996). Compared with IAB, OIB and WPB show no HFSE depletion (and sometimes enrichment) relative to REE

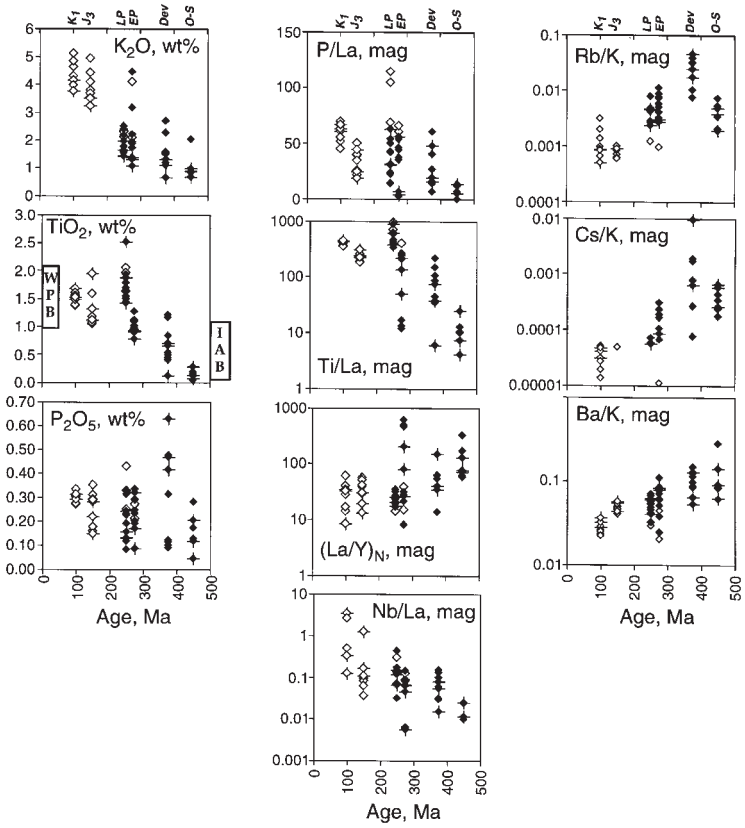
K1 J3
LP EP
Dev
O-S
K2O, wt%
TiO2, wt%
WPB
IAB
P2O5, wt%
Age, Ma
P/La, mag
Ti/La, mag
(La/Y)N, mag
Nb/La, mag
Age, Ma
Rb/K, mag
Cs/K, mag
Ba/K, mag
Age, Ma

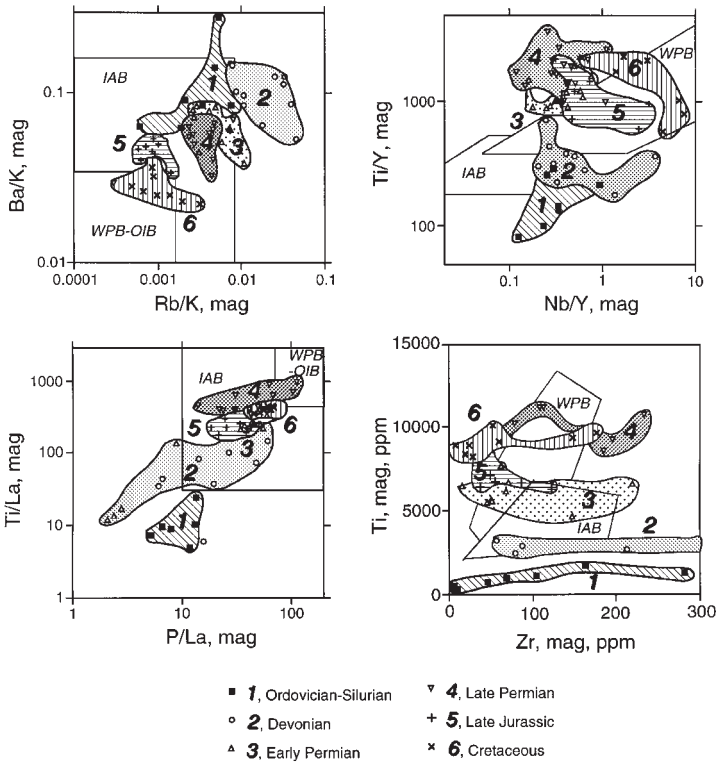
IAB
WPB-OIB
Ba/K, mag
Rb/K, mag
WPB
IAB
Ti/Y, mag
Nb/Y, mag
WPB
OIB
IAB
Ti/La, mag
P/La, mag
WPB
IAB
Ti, mag, ppm
Zr, mag, ppm
1, Ordovician-Silurian
2, Devonian
3, Early Permian
4, Late Permian
5, Late Jurassic
6, Cretaceous

and Y. In addition, LREE behave as LILE during subduction. They are shown to be preferentially leached from the slab with saline hydrothermal fluids and may enrich arc magmas in LREE and LILE (e.g. Keppler, 1996; Kosigo *et al.*, 1997; Tatsumi & Kosigo, 1997) relative to the MREE and HREE and Y. Hence the use of HFSE/LREE ratio (such as Ti/La vs P/La) should make the distinction even clearer.

Transbaikalian suites progressively increase in HFSE relative to Y (as a proxy for HREE) and especially Ti and P relative to La (LREE) with time. These element ratios and the absolute concentrations of Ti in later suites approach those in WPB–OIB in discrimination diagrams, hence confirming the progressive transition from IAB to OIB.

It is important to notice that the whole-rock trace element abundances in Late Cretaceous and younger volcanic suites including the Baikal rift volcanics (which are fresh and can be characterized using whole-rock techniques) closely match the trace element pattern of OIB (Fig. 12) (Yarmolyuk *et al.*, 1992; Kononova *et al.*, 1993). This confirms that the established Paleozoic and Early Mesozoic trends are developing toward OIB and a trace element signature characteristic of OIB occurs in the later suites (as in Fig. 12).

Spidergrams and comparison with modern volcanics from different environments

The reconstructed concentrations of trace elements were normalized to the primitive mantle composition (Sun & McDonough, 1989) and plotted on a spidergram (Fig. 12).

We also analyzed plagioclase megacrysts in basalts from different modern environments: Laki, Iceland, as an example of MORB; Mauna Loa, Hawaii, as an example of OIB; 12 Kurile island arc volcanics of various alkalinity (see Bindeman & Bailey, 1999) as examples of IAB; and 1944 lava flow of Vesuvius as an example of highly alkaline IAB-type volcanics (see Fig. 12a).

First we find that the plagioclase-based reconstructed spidergrams for these volcanics are similar in pattern to those of their respective average whole-rock equivalents from Sun & McDonough (1989), indicating that the plagioclase-based reconstructed patterns are not artifacts of the partition coefficients. Next, we use the reconstructed compositions of these modern volcanics, as well as published averaged composition of various OIB and IAB, to match the Transbaikalian spidergrams.

We found that highly alkaline IAB-type volcanics from Vesuvius and the Aeolian island arc (but not the less alkali-rich Kurile volcanics) match both the absolute concentrations and the zigzag pattern of the earlier Transbaikalian suites. The normalized reconstructed compositions of the studied Hawaiian rock, and the averaged published OIB, match most details of the later Transbaikalian suites. The reconstructed trace element pattern based on Icelandic plagioclases is low in absolute level of concentration and different in pattern. Therefore, most of Transbaikalian suites lie within the described trace element patterns of highly alkaline intraplate volcanics with IAB affinity, and OIB.

We next observe the systematic change in the normalized trace element pattern for different Transbaikalian suites. Ordovician–Silurian and Devonian suites exhibit a trace elemental zigzag pattern, more reminiscent of the above-mentioned present-day alkaline IAB: strongly enriched LILE, high Rb/K, Ba/K, Cs/K ratios, and low HFSE concentrations. The Early Cretaceous suite matches OIB trace element patterns. Younger suites—Late Cretaceous, Tertiary and Quaternary—are also typical OIBs, as revealed by whole-rock analyses (Kononova *et al.*, 1993) (Fig. 12c). Between these, Permian to Jurassic suites show similar IAB zigzag patterns, but with a steady increase in HFSE, and decreasing Rb/K, Ba/K and Cs/K ratios. This seems to reflect a tendency towards OIB trace element patterns.

DISCUSSION

Evolution of basic magmatism during cratonization

The use of plagioclase cores allows us to retrieve a primitive trace element signature of primitive basic magma as a window to the mantle underneath the evolving craton. It is particularly important given the role of basic magmas in generating the enormous volumes of syenites and granites throughout the Paleozoic, and the fact that the exposed coeval primitive mafic rocks are extremely sparse in Transbaikalia and other areas of orogenic and anorogenic magmatism.

The chemical trends described above allow us to discuss the evolution of basic magmatism in a single lithospheric

Fig. 11. Reconstructed trace element concentrations and ratios for primary basaltic magmas of Transbaikalia, relevant to geodynamic interpretations. WPB, within-plate basalt; OIB, ocean island basalt; IAB, island arc basalt. Fields of modern WPB–OIB and IAB on Ti–Y and Ti/Y vs Nb/Y diagrams are from Pearce & Cann (1973) and Pearce (1982), respectively. A temporal trend from IAB toward WPB–OIB should be noted. Ranges of Ba/K, Rb/K, Ti/La, P/La in OIB and IAB are from McDonough *et al.* (1992), Sun & McDonough (1989), White & Patchett (1984), Hickey *et al.* (1986) and Johnson & Arculus (1978), respectively. La/Y was normalized to the chondrite value from Sun & McDonough (1989). (See Fig. 10 for symbols.)

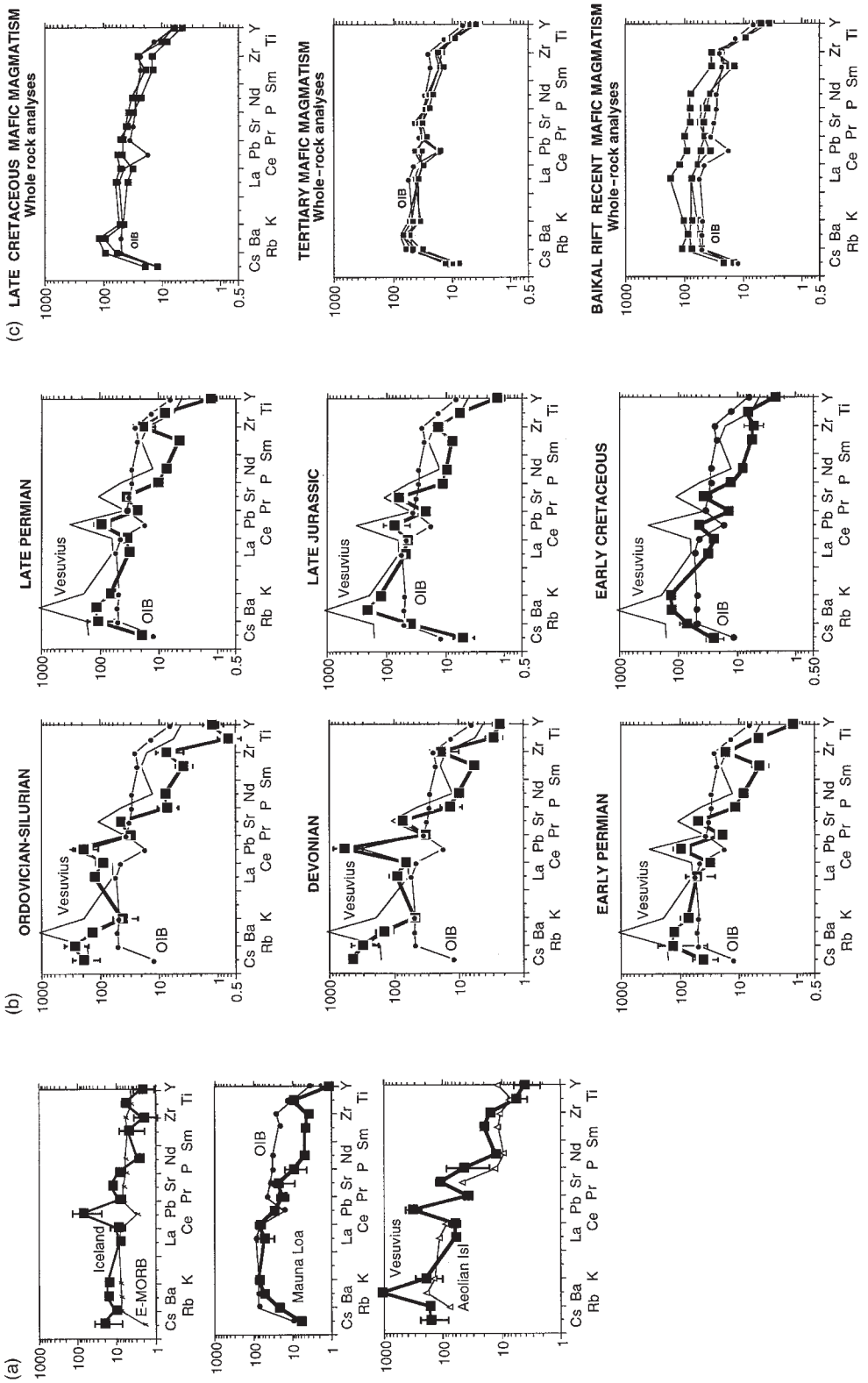
(a)
Iceland
E-MORB
OIB
Mauna Loa
Vesuvius
Aeolian Isl
(b)
ORDOVICIAN-SILURIAN
LATE PERMIAN
DEVONIAN
LATE JURASSIC
EARLY CRETACEOUS
EARLY PERMIAN
Vesuvius
OIB
(c)
LATE CRETACEOUS MAFIC MAGMATISM
Whole rock analyses
TERTIARY MAFIC MAGMATISM
Whole-rock analyses
BAIKAL RIFT RECENT MAFIC MAGMATISM
Whole-rock analyses
Cs Ba Rb K La Pb Sr Nd Ce Pr P Sm Zr Y Ti

block during 400 my after collision: a history of progressive cratonization.

Geological evidence for an intracratonic tectonic environment of magmatism since at least Devonian times (e.g. Gordienko, 1987; Zonenshain *et al.*, 1990), as well as a clear anorogenic nature of coeval silicic plutonism (e.g. Wickham *et al.*, 1995, 1996) make us search for an explanation of the sources of the basic magma. The critical observations include: (1) the decrease in overall magmatic volumes; (2) the transition from island-arc trace elemental pattern of the Early Paleozoic suites to clear OIB signature of Mesozoic–Cenozoic suites (see above); (3) the parallel decrease in $\delta^{18}O$ (e.g. Fig. 5).

The arc-related trace elemental signature in post-collisional environments may be a result of millions of years of pre-existing subduction underneath the Siberian craton in Precambrian and Early Paleozoic times. It suggests that, during this subduction, the subcontinental lithosphere under Transbaikalia became enriched with subduction-related components. The observed decrease in Rb, LREE and hydrophile element (Li, B, and Pb) concentrations notably reflects depletion and eventual exhaustion of a subduction-related component through time. As a result, the island arc-related trace elemental signature inherited from hundreds of millions of years of subduction progressively faded through the course of removal of melt during each stage of basic magmatism. The compositional evolution correlates with the overall decrease in magmatic volumes, although the exact proportions of each are difficult to determine. On the other hand, the concentrations of HFSE (Nb, Ti and P) increased with time to the level of OIB. This transition indicates that not only was sublithospheric mantle involved in partial melting, but also it supplied some components, and especially K with time. Despite the overall decrease in magmatic volumes, the relative role of sublithospheric mantle in melt generation increased with time, and when the lithosphere was exhausted, the basic magmatism became sublithospheric mantle dominated.

The progressive decrease in LILE, LREE, and volatile elements suggests a similar trend for H_2O, which could cause an increase in the mantle solidus temperature, and possibly a deepening of the melting zone. These changes correspond to an increase in mantle viscosity and perhaps thickening of the lithosphere, a possible aspect of cratonization (Pollack, 1986).

The reason for $\delta^{18}O$ decrease from 7·8‰ in Ordovician–Silurian to ~6‰ in Cretaceous (see Fig. 5) and Cenozoic time (e.g. Pokrovsky, 1991) may reflect a similar trend. The temporal evolution of $\delta^{18}O$ composition of the mantle source in the continental lithosphere may result from preferential removal of more volatile-rich, more fusible and more $\delta^{18}O$-rich component during these melting episodes. It leads to the temporal exhaustion of this component in the lithospheric mantle, which becomes progressively replaced by more $\delta^{18}O$-poor sublithospheric OIB component. As a result, younger suites are more and more depleted in $\delta^{18}O$.

Increases with time in both K_2O and HFSE similarly characterize other anorogenic provinces: Brazil (Dal'Agnol *et al.*, 1987), the Arabian–Nubian shield (Abdel-Rahman, 1995) and the North American anorogenic provinces (Windley, 1984; Ramo, 1991; Anderson & Morrison, 1992). The observed geochemical trends appear characteristic of orogenic to anorogenic magmatism during cratonization.

Tectonic implications

The chemical trends of evolution of basic magmatism allow speculation on the tectonic evolution of the central part of Eurasia for the last 400 my. Formation of the huge Angaro–Vitim batholith in Ordovician–Silurian time was a result of a large-scale collisional event (Gordienko, 1987; Zonenshain *et al.*, 1990; Litvinovsky *et al.*, 1994) that plausibly produced a body of thickened continental crust over the vast area of southern Siberia. A mountain plateau comparable in size with Tibet, and isostatically compensating lithospheric roots, formed as a result of this collision. As is accepted in recent models on collisional magmatism (Willett & Beaumont, 1994), conductive heating of these roots, additionally heated by radioactive decay of the U, Th, and K in thickened continental crust, could be the mechanism for such a great scale of remelting and formation of the Angaro-Vitim batholith. In addition, fast erosion of the uplifted area of thickened continental crust could have resulted in pressure release in the crustal roots, causing adiabatic melting of both the crust and the lithospheric mantle.

Fig. 12. Trace element signature of Transbaikalian mafic rocks of different ages. (a) Spidergrams of the plagioclase-based reconstructed compositions of parental basalts in Iceland, Hawaii and Vesuvius in comparison with the E-MORB (mid-ocean ridge basalt), OIB, and Aeolian calc-alkaline basalts (Sun & McDonough, 1989). (b) Reconstructed spidergram for primary basaltic magmas of Transbaikalia. Solid squares and thick lines represent averaged reconstructed plagioclase-based concentrations of trace elements of each suite. Thinner lines are averaged reconstructed ion microprobe analyses based on plagioclases from Vesuvius (this study). Thinner line with circles are OIB from Sun & McDonough (1989). The reconstructed compositions were normalized using primitive mantle concentrations from Sun & McDonough (1989). (c) Whole-rock spidergrams for Late Cretaceous–Cenozoic basalts.

Therefore, both radioactive heating and adiabatic melting are believed to be the most plausible mechanisms for the silicic and basic magmatism not only during the Ordovician–Silurian collisional and rebounding stages, but also throughout the Paleozoic history. The decaying volumes of magmatism since Ordovician–Silurian time are consistent with this interpretation.

The role of subduction underneath the newly accreted terrane in the later Paleozoic history is unclear. On the one hand, the trend of trace elements in the reconstructed basic magma from Devonian to Jurassic time indicates that a subduction-related component was involved in magma genesis. On the other hand, we observe depletion of this component with time, and a gradual increase in OIB component (see Figs 11 and 12). It could be that no additional subduction took place underneath Siberia since Devonian time and that the subduction-related component perished since then. In this view, the observed decrease in the subduction-related component with time is associated with devolatilization of the mantle sources.

We view the southern margin of the Siberian craton after the Ordovician–Silurian collision as a passive continental margin. Subduction could have occurred south of this margin in the ocean-surrounded island arcs (e.g. Sengor & Natal'in, 1996); the direction of subduction could be either to the north underneath these arcs, and/or to the south, underneath the Southern Mongolia and China blocks. After these blocks had collided with Siberia and the Mongol–Okhotsk ocean was closed, the intracontinental, OIB-type magmatism in Transbaikalia reflected effective depletion of the lithospheric mantle in arc-related components. This view is consistent with the anorogenic nature of silicic magmatism since Late Paleozoic time (Wickham *et al.*, 1995, 1996). Extension and rifting started in Late Permian time and were probably associated with decompression melting of the sublithospheric mantle. Extension culminated in the Tertiary opening of the Baikal rift. Cenozoic rifting is concordant with the expected stress, imposed by the India–Asia collision (Zonenshain *et al.*, 1990), whereas Permian and Early Mesozoic rifts could be related to similar earlier collisions of microcontinents in Southeast Asia. The origin of rifting and associated volcanics is under debate. Models include: (1) passive rifting (Zonenshain *et al.*, 1990; Rasskazov, 1994); (2) the hotspot and asthenospheric diapir model (Kiselev & Popov, 1992; (3) a combination of these two (Yarmolyuk *et al.*, 1992). Given the tectono-magmatic evolution picture presented above, we prefer a passive-rifting model of steadily cooling and cratonizing lithosphere. This magmatic progression, from calc-alkaline to alkaline series, is recorded world wide (e.g. Windley, 1984, 1993; Bonin, 1987) and is attributed to the thermal evolution of the lithosphere (e.g. Pollack, 1986). It does not exclude, however, superposition of local short-lived hotspots, such as the southern Baikal one (Yarmolyuk *et al.*, 1992).

To constrain tectono-magmatic evolution in greater detail requires knowledge of the many factors governing the largely cryptic processes of cratonization. These include the temporal drift of the cratonizing lithosphere over sublithospheric mantle of varying composition, degrees of melting and temperatures (e.g. hotspots), and 'mantle extrusion' (e.g. Hoang & Flower, 1998). Therefore, the role of sublithospheric mantle is largely hidden. The other unknown factor in a geochemical budget is the thickness and volume of the cratonizing lithospheric mantle, which can change as a result of both mechanical delamination after collision, and consequent slow temporal evolution and depletion.

Concluding remarks

Ion microprobe study of surviving primary plagioclase cores serves as a new tool in basic magma petrogenesis and provides a better insight into mantle magmatism. It provides a view of the early stages of magma evolution by overcoming the superimposed effects of fractionation, mixing and secondary alteration in primitive stage magma evolution in more detail than simple whole-rock analysis. Furthermore, it adequately constrains the trace element signature on temporal trends of basic magmatism, and fingerprints its tectonic position. In combination with oxygen isotopes, this study provides a clearer understanding of geochemical trends during the transformation from a mountain plateau region to a stable cratonic region.

ACKNOWLEDGEMENTS

The work is a part of the Ph.D. thesis of I.N.B. The authors are grateful to A. N. Zanvilevich, B. A. Litvinovsky and V. A. Pervov for discussions, field assistance and donation of some samples; Tosh Mayeda for help with some oxygen isotope analyses; and Ian Steele for help with electron probe. Formal reviews by John Valley, Martin Flower and Pavel Kepezhinskas, and informal reviews by Fred Anderson, Dave Rowley, Bob Clayton and a number of University of Chicago colleagues are greatly appreciated. This work was supported by NASA Grant NAGW-3384 to A.M.D., NSF Grant EAR-9417787 to A. T. Anderson, and NSF Grant EAR-9304080 to S.M.W.

REFERENCES

Abdel-Rahman, M. A-F. (1995). Tectonic–magmatic stages of shield evolution; the Pan-African belt in northeastern Egypt. *Tectonophysics* **242,** 223–240.

Anderson, J. L. & Morrison, J. (1992). The role of anorogenic granites in the Proterozoic crustal development of North America. *Developments in Precambrian Geology* **10,** 263–299.

Barker, F., Wones, D. R., Sharp, W. N. & Desborough, G. A. (1975). The Pikes Peak Batholith, Colorado Front Range, and a model for the origin of the gabbro–anorthosite–syenite–potassic granite suite. *Precambrian Research* **2,** 97–160.

Bindeman, I. N. (1998). Trace element partitioning between plagioclase feldspar and melt: a study of experiments and applications to magmatic evolution. Ph.D. dissertation, University of Chicago.

Bindeman, I. N. & Bailey, J. C. (1999). Trace elements in anorthite megacrysts from the Kurile island arc: a window to across-arc geochemical variations in magma compositions. *Earth and Planetary Science Letters* (in press).

Bindeman, I. N., Davis, A. M. & Drake, M. J. (1998). An ion microprobe study of plagioclase–basalt partition experiments at natural concentration levels of trace elements. *Geochimica et Cosmochimica Acta* **62,** 1175–1193.

Blundy, J. D. & Shimizu, N. (1991). Trace element evidence for plagioclase recycling in calc-alkaline magmas. *Earth and Planetary Science Letters* **102,** 178–197.

Blundy, J. D. & Wood, B. J. (1991). Crystal-chemical control on the partitioning of Sr and Ba between plagioclase feldspar, silicate melts, and hydrothermal solutions. *Geochimica et Cosmochimica Acta* **55,** 193–209.

Bonin, B. (1987). From orogenic to anorogenic magmatism: a petrological model for the transition calc-alkaline–alkaline complexes. *Revista Brasiliera de Geociencias* **17,** 366–371.

Brady, J. B. (1995). Diffusion data for silicate minerals, glasses, and liquids. In: Ahrens, T. J. (ed.) *Mineral Physics and Crystallography, a Handbook of Physical Constants. American Geophysical Union Reference Shelf* **2,** 269–290.

Cherniak, D. J. (1995). Diffusion of lead in plagioclase and K-feldspar: an investigation using Rutherford backscattering and resonant nuclear reaction analysis. *Contributions to Mineralogy and Petrology* **120,** 358–371.

Cherniak, D. J. & Watson, E. B. (1992). A study of Sr diffusion in K-feldspar, Na–K feldspar and anorthite using Rutherford backscattering spectroscopy. *Earth and Planetary Science Letters* **113,** 411–425.

Criss, R. E. & Taylor, H. P., Jr (1986). Meteoric–hydrothermal systems. In: Valley, J. W., Taylor, H. P., Jr & O'Neil, J. R. (eds) *Stable Isotopes in High Temperature Geological Processes. Mineralogical Society of America, Reviews in Mineralogy* **16,** 373–424.

Dal'Agnol, R., Bettencourt, J. S. & Jorge-Joao, X. D. S. (1987). Granitogenesis of the Northern Brazilian Region: a review. *Revista Brasiliera de Geociencias* **17,** 382–403.

Davidson, J. P. & Tepley, F. J. III (1981). Recharge in volcanic systems: evidence from isotope profiles of phenocrysts. *Science* **275,** 826–829.

DePaolo, D. J. (1981). Trace element and isotopic effects on combined wallrock assimilation and fractional crystallization. *Earth and Planetary Science Letters* **53,** 189–202.

Frost, T. P. & Mahood, G. A. (1987). Field, chemical, and physical constraints on mafic–felsic magma interaction in the Lamarck Granodiorite, Sierra Nevada, California. *Geological Society of America Bulletin* **99,** 272–291.

Furman, T. & Spera, F. G. (1985). Co-mingling of acid and basic magma with implications for the origin of mafic I-type xenoliths; field and petrochemical relations of an unusual dike complex at Eagle Lake, Sequoia National Park, California, USA. *Journal of Volcanology and Geothermal Research* **24,** 151–173.

Giletti, B. J. (1994). Isotopic equilibrium/disequilibrium and diffusion kinetics in feldspars. In: Parson, I. (ed.) *Feldspars and their Reactions. NATO ASI Series 421.* Boston: Kluwer Academic, pp. 351–382.

Giletti, B. J. & Shanahan, T. M. (1997). Alkali diffusion in plagioclase feldspar. *Chemical Geology* **139,** 3–20.

Gordienko, I. V. (1987). *Paleozoic Magmatism and Geodynamics of the Central Asian Fold Belt* (in Russian). Moscow: Nauka, 238 pp.

Harmon, R. S. & Hoefs, J. (1995). Oxygen isotope heterogeneity of the mantle, deduced from global systematics of basalts from different tectonic settings. *Contributions to Mineralogy and Petrology* **120,** 95–114.

Hickey, R. L., Frey, F. A. & Gerlach, D. C. (1986). Multiple sources for basaltic arc rocks from the SVZ of the Andes: trace element and isotopic evidence for contribution from subducted oceanic crust, mantle, and continental crust. *Journal of Geophysical Research* **91,** 5963–5983.

Hoang, N. & Flower, M. F. J. (1998). Petrogenesis of Cenozoic basalts from Vietnam: implications for origin of a 'Diffusive Igneous Province'. *Journal of Petrology* **39,** 369–395.

Johnson, R. W. & Arculus, R. J. (1978). Volcanic rocks of the Witu islands, Papua New Guinea: the origin of magmas above the deepest part of the New Britain Benioff zone. *Bulletin of Volcanology* **41,** 609–655.

Keppler, H. (1996). Constraints from partitioning experiments on the composition of subduction zone fluids. *Nature* **380,** 237–240.

Kiselev, A. I. & Popov, A. M. (1992). Asthenospheric diapir beneath the Baikal rift: petrological constraints. *Tectonophysics* **208,** 287–295.

Kononova, V. A., Keller, Y. & Pervov, V. A. (1993). Continental basaltic volcanism and geodynamic evolution of Baikal–Mongol region. *Petrology* **1,** 152–170.

Kosigo, T., Tatsumi, Y. & Nakano, S. (1997). Trace element transport during dehydration processes in the subducted oceanic crust: 1. Experiments and implications for the origin of ocean island basalts. *Earth and Planetary Science Letters* **148,** 193–203.

Kyser, T. K. (1986). Stable isotopes variations in the mantle. In: Valley, J. W., Taylor, H. P., Jr & O'Neil, J. R. (eds) *Stable Isotopes in High Temperature Geological Processes. Mineralogical Society of America, Reviews in Mineralogy* **16,** 141–162.

Kyser, T. K. (1993). Stable isotopes in the continental lithospheric mantle. In: Menzies, M. (ed.) *Continental Mantle.* Oxford: Clarendon Press, pp. 127–156.

Leontiev, A. N., Litvinovsky, B. A., Gavrilova, S. P. & Zakharov, A. A. (1981). *Paleozoic Granitoid Magmatism of the Central Asian Fold Belt* (in Russian). Moscow: Nauka.

Litvinovsky, B. A. & Zanvilevich, A. N. (1998). Compositional trends of silicic and mafic magmas formed in the course of the mobile belt evolution: petrogenetic aspects. *Geologiya i Geofizika* **39,** 157–177.

Litvinovsky, B. A., Zanvilevich, A. N. & Wickham, S. M. (1994). The Angaro–Vitim batholith, Transbaikalia: structure, petrology and petrogenesis. *Geologiya i Geofizika* **35,** 218–234.

McDonough, W. F., Sun, S.-S., Ringwood, A. E., Jagoutz, E. & Hofmann, A. W. (1992). Potassium, rubidium and cesium in the Earth and Moon and the evolution of the mantle of the Earth. *Geochimica et Cosmochimica Acta* **56,** 1001–1012.

McKay, G. A. (1989). Partitioning of rare earth elements between major silicate minerals and basaltic melts. In: Lipin, B. R. & McKay, G. A. (eds) *Geochemistry and Mineralogy of Rare Earth Elements. Mineralogical Society of America, Reviews in Mineralogy* **21,** 45–77.

Morse, S. A. (1984). Cation diffusion in plagioclase feldspar. *Science* **225,** 504–505.

Neymark, L. A., Rytsk, Y. Y., Rizvanova, N. G. & Gorokhovsky, B. M. (1993). On the polychronous nature of the Angaro–Vitim batholith according to U–Pb dating of zircon and sphene. *Doklady Akademii Nauk* **333,** 635–637.

Nie, S., Rowley, D. B. & Ziegler, A. M. (1990). Constraints on the locations of Asian microcontinents in Palaeo-Tethys during the Late Palaeozoic. In: McKerrow, W. S. & Scotese, C. R. (eds) *Palaeozoic*

Palaeogeography and Biogeography. Geological Society, London, Memoir **12,** 397–409.

Noll, P. D., Jr, Newsom, H. E., Leeman, W. P. & Ryan, J. G. (1996). The role of hydrothermal fluids in the production of subduction zone magmas: evidence from siderophile and chalcophile elements and boron. *Geochimica et Cosmochimica Acta* **60,** 587–611.

Pearce, J. A. (1982). Trace elements characteristics of lavas from destructive plate boundaries. In: Thorpe, R. S. (ed.) *Andesites*. Chichester: John Wiley, pp. 525–548.

Pearce, J. A. & Cann, J. R. (1973). Tectonic setting of basic volcanic rocks determined using trace element analyses. *Earth and Planetary Science Letters* **19,** 290–300.

Phinney, W. C. (1992). Partition coefficients for iron between plagioclase and basalts as a function of oxygen fugacity; implication for Archean and lunar anorthosites. *Geochimica et Cosmochimica Acta* **56,** 1885–1895.

Pokrovsky, B. G. (1991). Isotope characteristics of alkaline extrusive rocks of Udokansky ridge (in Russian). *Geokhimiya* **7,** 995–1003.

Pollack, H. M. (1986). Cratonization and thermal evolution of the mantle. *Earth and Planetary Science Letters* **80,** 175–182.

Ramo, O. T. (1991). Petrogenesis of the Proterozoic rapakivi granite and related basic rocks of southeastern Fennoscandia: Nd and Pb isotopic and general geochemical constraints. *Bulletin of the Geological Society of Finland* **355,** 1–166.

Rasskazov, S. V. (1993). *Magmatism of Baikal Rift System* (in Russian). Novosibirsk: Nauka, 215 pp.

Rasskazov, S. V. (1994). Magmatism related to the eastern Siberia rift system and the geodynamics. *Bulletin des Centres de Recherches Exploration-Production Elf-Aquitaine* **18,** 437–452.

Sengor, A. M. C. & Natal'in, B. A. (1996). Paleotectonics of Asia: fragments of a synthesis. In: Yin, A. & Harrison, M. T. (eds) *The Tectonic Evolution of Asia*. Cambridge: Cambridge University Press, pp. 486–580.

Sharkov, Ye. V. & Bindeman, I. N. (1990). Petrology of xenolith-bearing basalts from the Baikal-rift zone: Tunka, Dzhida and Vitim areas. *Volcanology and Seismology* **12,** 443–459.

Shimizu, N. & Hart, S. R. (1982). Application of the ion microprobe to geochemistry and cosmochemistry. *Annual Review of Earth and Planetary Sciences* **10,** 483–526.

Singer, B. S., Dungan, M. A. & Layne, G. D. (1995). Textures and Sr, Ba, Mg, Fe, K, and Ti compositional profiles in volcanic plagioclase: clues to the dynamics of calc-alkaline magma chambers. *American Mineralogist* **80,** 776–798.

Smith, J. V. & Brown, W. L. (1988). *Feldspar Minerals, Vol. 1*. Berlin: Springer-Verlag.

Sun, S.-S. & McDonough, W. F. (1989). Chemical and isotopic systematics of oceanic basalts: implications for mantle composition and processes. In: Saunders, A. D. & Norry, M. J. (eds) *Magmatism in the Ocean Basins. Geological Society, London, Special Publications* **42,** 313–345.

Tatsumi, Y. & Kosigo, T. (1997). Trace element transport during dehydration processes in the subducted oceanic crust: 2. Origin of chemical and physical characteristics in arc magmatism. *Earth and Planetary Science Letters* **148,** 207–221.

Tatsumi, Y., Hamilton, D. L. & Nesbitt, R. W. (1986). Chemical characteristics of fluid phase released from a subducted lithosphere and origin of arc magma; evidence from high-pressure experiments and natural rocks. *Journal of Volcanology and Geothermal Research* **29,** 293–309.

White, W. M. & Patchett, P. J. (1984). Hf–Nd–Sr isotopes and incompatible element abundances in island arcs: implications for magma origins and crust–mantle evolution. *Earth and Planetary Science Letters* **67,** 167–185.

Wickham, S. M., Litvinovsky, B. A., Zanvilevich, A. N. & Bindeman, I. N. (1995). Geochemical evolution of Phanerozoic magmatism in Transbaikalia, East Asia: a key constraint on the origin of K-rich silicic magmas and the process of cratonization. *Journal of Geophysical Research* **100,** 15641–15654.

Wickham, S. M., Alberts, A. D., Zanvilevich, A. N., Litvinovsky, B. A., Bindeman, I. N. & Schauble, E. A. (1996). A stable isotope study of anorogenic magmatism in East Central Asia. *Journal of Petrology* **37,** 1068–1095.

Willett, S. D. & Beaumont, C. (1994). Subduction of Asian lithospheric mantle beneath Tibet inferred from models of continental collision. *Nature* **368,** 642–645.

Wilson, B. M. (1989). *Igneous Petrogenesis*. London: Unwin Hyman, 466 pp.

Windley, B. F. (1984). *The Evolving Continents*. New York: John Wiley, 399 pp.

Windley, B. F. (1993). Proterozoic anorogenic magmatism and its orogenic connections. *Journal of the Geological Society, London* **150,** 39–50.

Yarmolyuk, V. V., Kovalenko, V. I. & Bogatikov, O. A. (1992). The south Baikal mantle hot spot and its role in the development of the Baikal rift zone. *Transactions of the Russian Academy of Sciences, Earth Science Section* **312,** 187–191.

Zanvilevich, A. N. & Litvinovsky, B. A. (1991). Coexisting magmas of contrasting composition in gabbro–granite series in mobile belts. In: *Geodynamic Evolution and Main Sutures of the Paleo-Asian Ocean. Report 2, International Geological Correlation Program Project* **238,** 97–100.

Zanvilevich, A. N., Litvinovsky, B. A. & Andreev, G. V. (1985). *Mongolia–Transbaikalian Granitoid Province* (in Russian). Moscow: Nauka, 232 pp.

Zinner, E. & Crozaz, C. (1986). A method for the quantitative measurement of rare earth elements in the ion microprobe. *International Journal of Mass Spectrometry and Ion Physics* **69,** 17–38.

Zonenshain, L. P., Kuzmin, M. I. & Natapov, L. M. (1990). *Geology of the USSR: a Plate Tectonic Synthesis. American Geophysical Union Geodynamics Series* **21,** 242 pp.